DEMONSTRATION AT AN OFFSHORE FOUNDATION

Why this location

The Blue Accelerator provides an offshore test site with much easier accessibility than an actual offshore wind turbine foundation. The latter, or at least the one Sirris has access through via a partnership with an offshore windfarm operator, is located 30km offshore. This provides significant practical challenges in case there are technical issues, but also has large costs associated to it (renting of vessels, additional safety personnel, gear, etc.).

In a first stage of testing, the Blue Accelerator provides a very good test location with conditions very similar to those at an actual windfarm. The salinity is higher than in a harbour, there are additional wave loads and aeration of the water, the marine growth (fouling) is similar, there are high and low tides and there are similar water movements and flows. The demo results even indicate that the situation at the Blue Accelerator may even be more aggressive than that found further from shore.

The biggest advantage of the Blue Accelerator is its proximity to the harbour of Ostend. It's only a 10min trip by boat. In case of technical malfunctions and other challenges associated with working in an extremely aggressive environment this is certainly no luxury and allows much more options for trouble shooting. This has proven to be indispensable in the current stage of development of the sensor system.

Baseline/starting situation

The baseline information given below in this section is largely based on the 'Environmental Effects Report' for the installation of the Blue Accelerator, as well as data obtained from the Flanders Marine Institute[1]. More specifically, conductivity and temperature data from measuring station 130 is given below in Figure 2.

[1] Flanders Marine Institute (VLIZ), Belgium (2020): LifeWatch observatory data: nutrient, pigment, suspended matter and secchi measurements in the Belgian Part of the North Sea. https://doi.org/10.14284/441. Accessed on 02/05/2023 through the LifeWatch Data Explorer / lwdataexplorer R package.

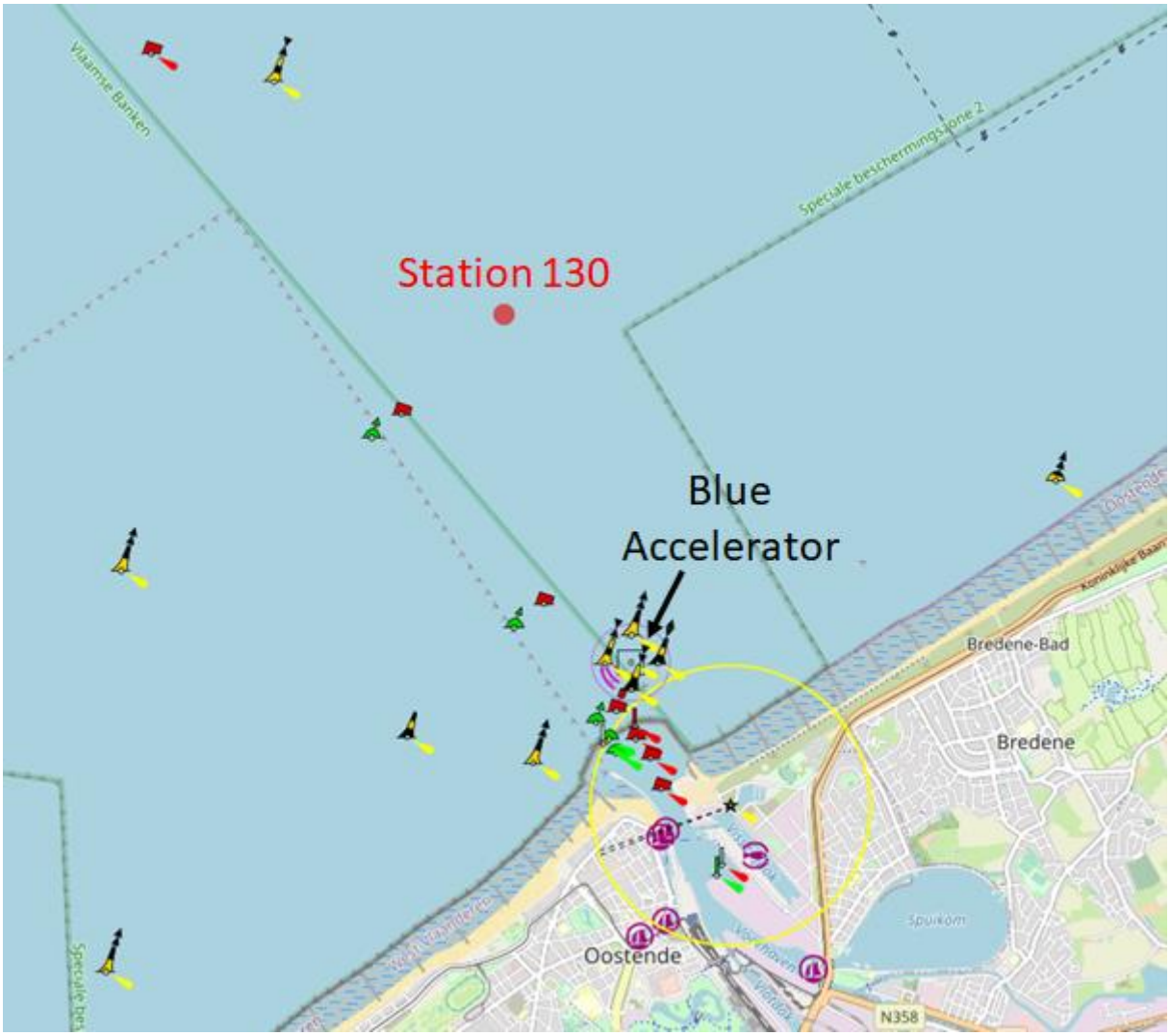

Figure 1: Location of the Blue Accelerator and measuring station 130 (red dot) of the Flanders Marine Institute.

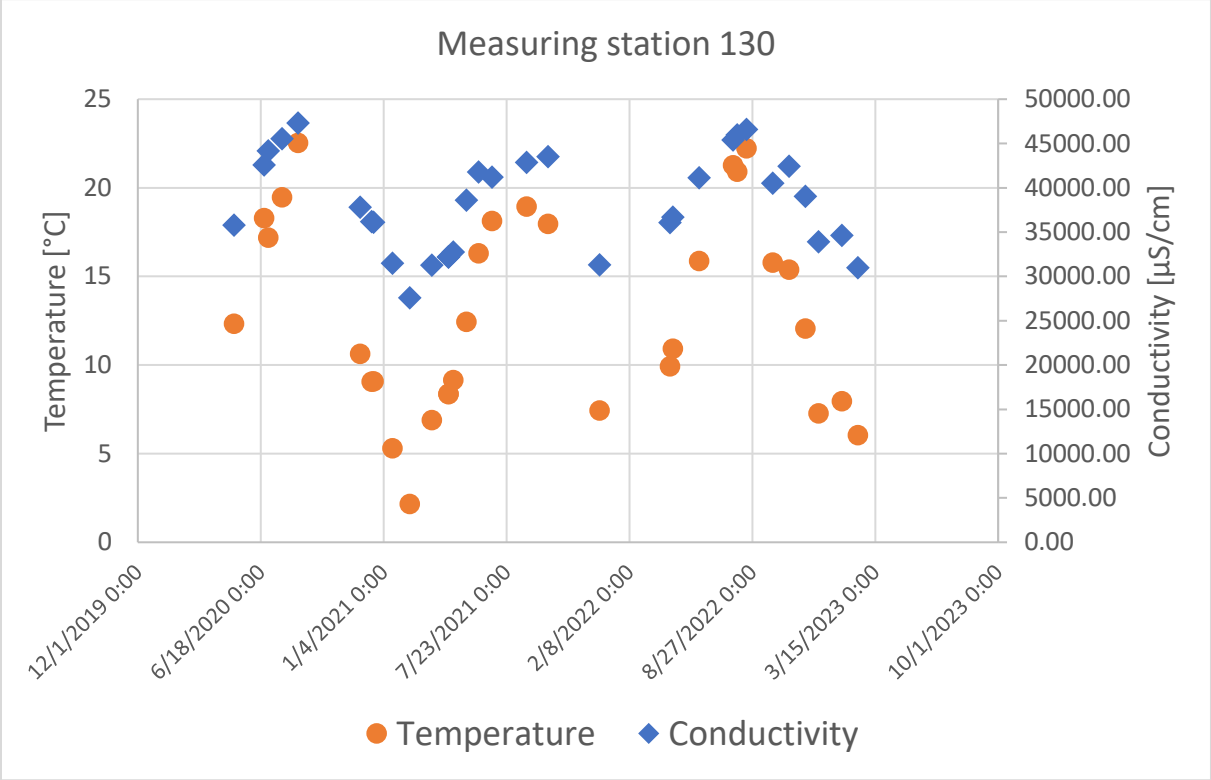

Figure 2: Temperature and conductivity data collected by the Flanders Marine Institute.

Temperature

The average water temperature in the Belgian part of the North Sea is around 11 °C. Seasonal variations occur with an order of magnitude of 8 to 9°C compared to the mean temperature, with the largest variations being observed in the first months of the year. Seawater temperature has an interannual variability of 1 to 4°C (Ruddick & Lacroix, 2006). Data from measuring station 130 of the Flanders Marine Institute is given in Figure 2.

Conductivity and Salinity

Salinity in the Belgian part of the North Sea is around 31 - 35 PSU (OSPAR, 2000; FOD Volksgezondheid, Veiligheid van de Voedselketen en Leefmilieu – DG Leefmilieu, 2010). There is a slight seasonal variation due to the influence of river inflow. At the project area, the average salinity is about 33 PSU (≈33000 mg/l). Conductivity data from measuring station 130 of the Flanders Marine Institute is given in Figure 2.

Dissolved Oxygen

The North Sea is typically well mixed due to a limited depth and significant water movement. Oxygen saturation is therefore expected to be close to 100%.

pH

No exact historical data for the pH at the demo site was found. However, the Flanders Marine Institute indicates that the pH of the North Sea has an average value of 8 +/-0.5[2]. Broadly speaking, the pH of surface sea water is said to be in the range of 8.1-8.2.

Turbidity

The project area is located in a zone up to about 5 km offshore, characterised by high suspended matter (suspended material and phytoplankton). In this zone where a turbidity maximum occurs, the concentration of mineral and organic constituents (SPM, Suspended Particulate Matter) varies from 100 mg/l to several 1000 mg/l.

During storms, the concentration at the coast can exceed 1000 mg/l. The sand sediments quickly, but the silt remains in suspension for several hours. Further offshore, maximum concentrations are more likely to be around 300 mg/l but they occur only occasionally.

Vertical variations

Belgian waters are generally well vertically mixed. As a result, there are only limited vertical variations.

Corrosion rates

Typical seawater corrosion rates for carbon steels are in the range of 0.1-0.3 mm/yr. Different values can be found for different studies, in different locations and for different durations. As an example, see the table below from the work of J.P. Ault.

Environmental zone	Corrosion rate (mm/y)
Buried in soil	0.06-0.10
Submerged zone	0.10-0.20
Intermediate zone	0.05-0.25
Splash zone	0.20-0.40
Atmospheric zone	0.050-0.075

Source: J.P. Ault, The Use of Coatings for Corrosion Control on Offshore Oil Structures, J. Prot. Coatings Linings. 11 (2006) 42–46.

Description of the demo site

Location

The Blue Accelerator test site is located approximately 500m from the shore, in front of the harbour of Ostend, as is illustrated in Figure 3. A picture taken from the location indicated with the blue star is shown in Figure 4. A close-up picture of the Blue Accelerator test site is shown in Figure 5. The Blue Accelerator test site is owned and operated by POM West-Vlaanderen. More information on the Blue Accelerator can be found online (https://www.blueaccelerator.be/).

[2] http://www.vliz.be/cijfers_beleid/zeecijfers/main.php?id=1&sid=10

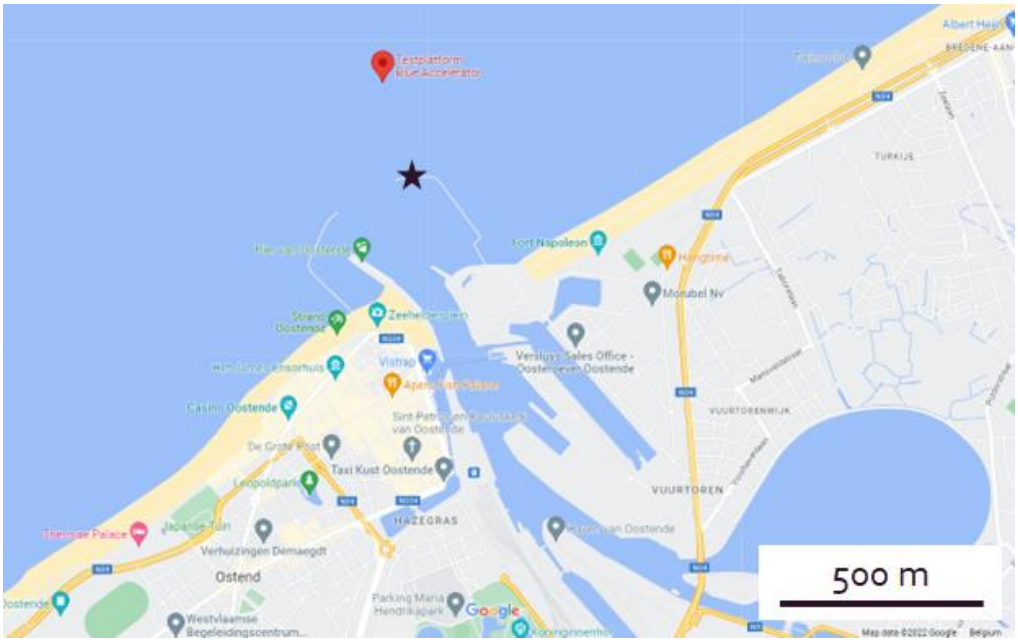

Figure 3: Location of the Blue Accelerator test site (indicated with red marker in the North Sea). Blue Star: location from which the picture in Figure 4 was taken. Source: Google© maps.

Figure 4: Picture of the Blue Accelerator, taken from the location indicated with the blue star in Figure 3.

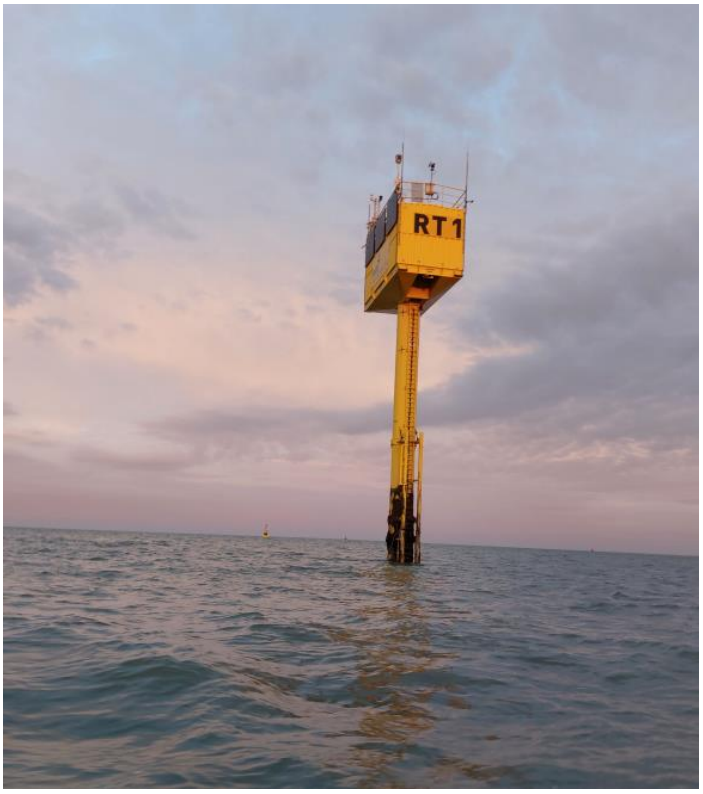

Figure 5: Close-up picture of the Blue Accelerator, taken during a trip to retrieve sensors.

The Blue Accelerator design is based on the principle of a monopile (MP) foundation. The MP itself is coated both internally and externally. Externally a Sacrificial Anode Cathodic Protection (SACP) system is also present. Internally no Cathodic Protection (CP) is present. The MP has no water refreshment holes, however there is a J-tube exiting the MP at the bottom. The J-tube is a tube through which cables can be guided from the inside to the outside of the structure. Where the J-tube passes through the MP wall, there is an opening that is not entirely sealed off. Internal water is thus possibly refreshed through the J-tube hole, although these may be blocked by fouling, resulting in a more stagnant volume of water inside the MP.

The structure can be accessed via a ladder at the boat landing (Figure 6, right). On the boat landing, at the land-side, a frame is installed on which sensors and test samples can be installed (Figure 6, left). The frame is installed such that the top of the frame is below LAT. The frame can be lifted up and down to take sensors out or put them in again. The inside of the MP is not sealed air-tight and can be accessed via a grating that can be lifted up. Sensors and samples can be lowered into the water on a rope.

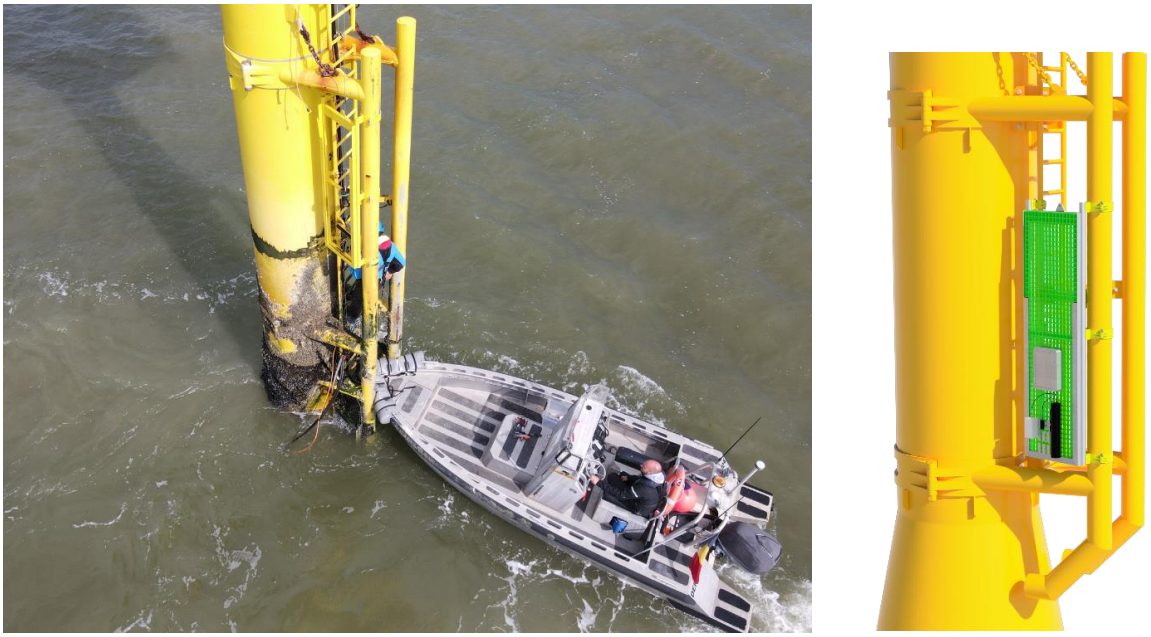

Figure 6: Left: Picture of installation crew accessing the structure via the boat landing and ladder to the platform. Right: 3D visualisation of the sensor frame installed on the boat landing.

SOCORRO test setup

For the purpose of the SOCORRO project two sets of sensors and corrosion coupons were installed, one on the inside of the monopile (referred to as BLUE1) and one on the outside of the monopile (referred to as BLUE2).

Internal setup (BLUE1)

On the inside of the MP, sensors were installed by hanging them off from a cable through the manhole. The sensors were positioned approximately at mid heigth of the water column (LAT reference) in such a way that the steel coupons and probes were touching the wall directly. The latter was realised by having a straight plastic frame behind them, which is at it sides touching the curved MP inner wall. In addition to the sensors and coupons shown in Figure 7, a multisensory probe was installed at the same height in the water column, but hanging from a separate cable.

The internal sensor set-up includes:

- 3x3 Corrosion coupons, S355 steel, surface condition: rolling skin, size: 80x20x3 mm
- 1 Multisensory probe Manta+30B from Eureka, procured by and with support from Royal Eijkelkamp. Measured parameters are: Dissolved Oxygen, Temperature, pH, Conductivity, ORP, Salinity, Chloride ion concentration. The sensors are protected by an anti-fouling Cu-shield.
- 1 Electrical Resistance (ER) probe from COSCASCO, model 620HD-1-S20, material type: K03005. Electrically insulated from the steel structure.
- 2 LPR sensor from C-Cube International. Materials S355 & Grade B. Electrically insulated from the steel structure.

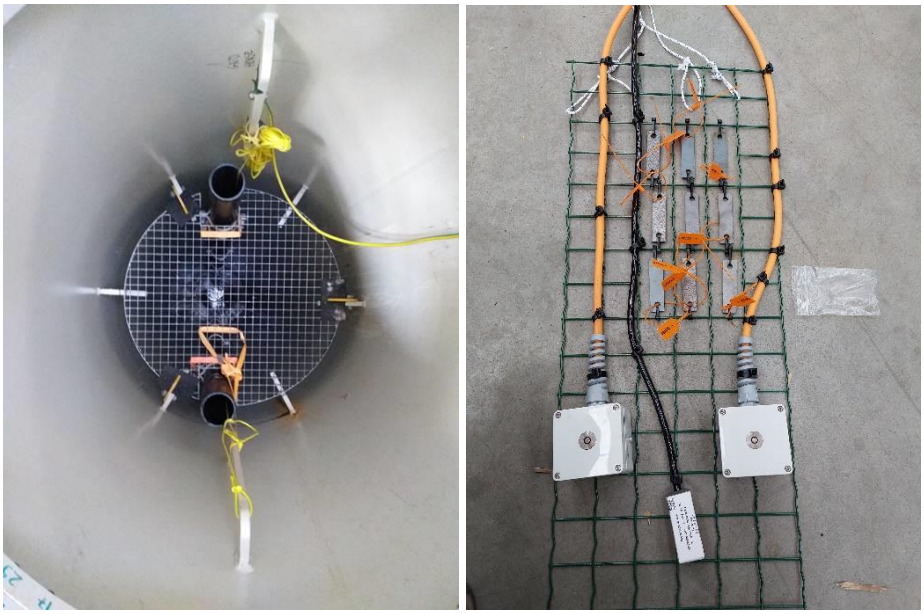

Figure 7: Left: Picture of the inside of the MP with safety grating. Right: picture of the frame with sensors and coupons attached, prior to installation.

External setup (BLUE2)

The external sensors were attached directly to the frame shown on (Figure 6, right). A multisensory probe was secured to the frame using 316 stainless steel cable binders. Corrosion coupons and corrosion sensors were fixed to the frame using plastic zip ties (black, UV resistant). The entire frame with sensors is shown on Figure 8, right.

The external sensor set-up includes:

- 3x3 Corrosion coupons, S355 steel, surface condition: rolling skin, size: 80x20x3 mm
- 1 Multisensory probe Manta+35A from Eureka, procured by and with support from Royal Eijkelkamp. Measured parameters are: Dissolved Oxygen, Temperature, pH, Conductivity, ORP, Salinity, Chloride ion concentration. The sensors are protected by an anti-fouling Cu-shield and a brush that moves over the sensors every 4 hours.
- 1 Electrical Resistance (ER) probe from COSCASCO, model 620HD-1-S20, material type: K03005. Electrically insulated from the steel structure.
- 1 LPR sensor from C-Cube International. Material: S355. Electrically insulated from the steel structure.
- Additional sensor data is available from Flanders Marine Institute VLIZ (not part of this project, can be found online at: https://rshiny.lifewatch.be/buoy-data/)

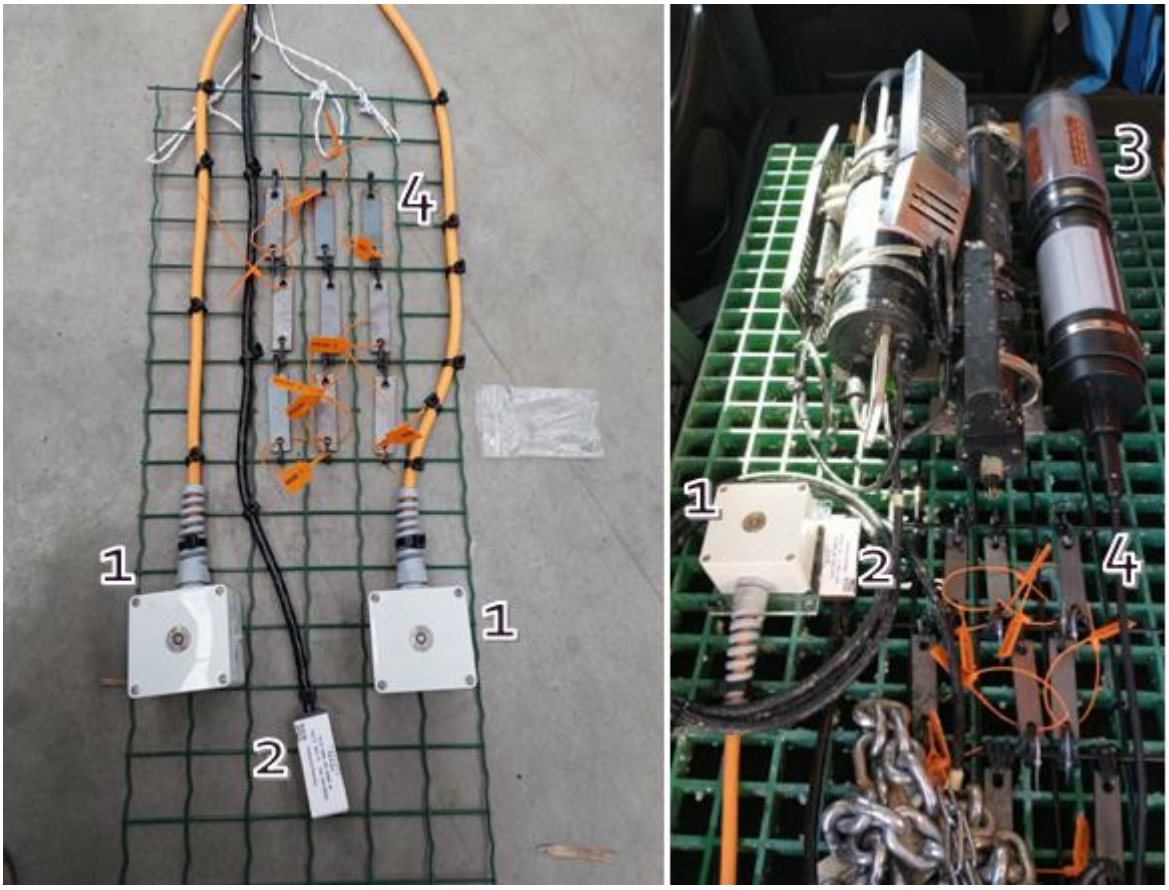

Figure 8: Left: Frame with corrosion coupons and sensors for installation on the inside of the MP. Right: Sensors and corrosion coupons installed on the outside of the MP. (1) C-Cube sensors, (2) COSASCO sensors, (3) Manta Multisensory probes and (4) corrosion coupons.

Timeline and technical remarks

Date	Description
16-17/5/2022	Installation of both internal and external sensor setup
16/07/2022	Start of anomalous readings on BLUE2 Dissolved oxygen sensor. Later inspection revealed corrosion on the sensor housing, probably leading to water ingress starting from this date. Also damage by large organisms cannot be excluded.
1-2/08/2022	Maintenance external sensors (BLUE2)
21-22/09/2022	Changed C-Cube counter electrode (CE): lead of the CE connected to the steel of the MP. (Data available from 23/9)
10/10/2022	Both multisensory probes retrieved for revision
31/11/2022	Frame lifted up to inspect for fouling and perform light cleaning
02/12/2022	Connection with data logger restored
25/01/2022	• Replaced multisensory probes, data connection issues were observed • Retrieved 3 coupons from the frame on the outside (BLUE2) • Verified COSASCO sensors with test probes. Both are measuring within specs.

08/02/2023	Manta35 (BLUE2, external) retrieved (no data). Observations: virtually no fouling present
09/02/2023	Interruption of data coming from Manta30 (BLUE1, internal)
20/02-27/02/23	Data logger was inactive during this period, no data received
09/03/2023	• Offshore inspection • Manta30 in good condition. Fuse of Data Acquisition System burned. Replaced fuse. Data connection restored. • Manta35 cable inspected. Cable broken. Damage marks point in direction of rubbing against location of hard biological fouling.

The summary of actions described in the timeline above, as well as the large periods of data interruption clearly show the difficulties associated with research and data collection in a very hostile environment. It should however be remarked that the data collected in the framework of the SOCORRO project is still the only in its kind, especially in terms of corrosion rate data. In addition, it can be remarked that in the same location and during the same time period, the Flanders Marine Institute was unable to perform water quality measurements due to similar technical problems, with sensors of a much higher cost. From this point of view, the results at the Blue Accelerator are in fact a huge success.

Nevertheless, from a technical point of view, there are a number of important points of learning, as summarised below.

1. Sensors for environmental parameters are designed for 1 month of uninterrupted operation. Within SOCORRO, we have taken efforts to expand this period, together with the chosen sensor supplier. Our results show we can now go up to 2-3 months depending on sensor and environment. This is already way past the expectations of the suppliers, but shows that longer periods of uninterrupted measurement are not yet possible without maintenance. The project thought us that such maintenance can take a long time, especially if hardware needs to be revised. It is therefore important to have at least two sensors per measurement location, so that a sensor can be exchanged and maintenance can be done at leisure. That would have resulted in less data interruption.
2. Although precautions were already taken to protect the sensors and cables from the action of waves and tidal currents. It is clear that the environment is even more aggressive than we anticipated and that special designed and armoured cables will be needed for long term operation.
3. Anti-fouling protection is critical and needs to be very robust to survive the aggressive environment. We learned that the used copper mesh needed to be fixed more securely than what was standard and that stronger materials are needed for the anti-fouling brush we applied. The supplier has already updated its design specs. We also learned that the brush alone does not suffice and in future work want to investigate the potential of UV light to further expand the operating window of the sensors.
4. There should be fail-saves and automated warnings to prevent loss of data in case of DAQ malfunction.

5. Measuring in an unmanned offshore location remains subject to the whims of nature and technology. Unforeseen situations must be expected. As an example, the wind turbine and solar panels that supply the Blue Accelerator with energy broke off during a storm, resulting in power shortages and loss of data. In an offshore environment, such unexpected situations cannot be avoided, even with the best preparation, and take more time to fix than onshore due to limited accessibility.

To clarify point 3, some pictures taken during the inspection of BLUE2 sensor on 10/10/2022 are shown in Figure 9. It is clear from picture 1 and 2 that the copper mesh which is meant to protect the sensors inside the protection cap is missing.

Figure 9: [1] Picture of a new protection cap with copper mesh present (fortified version for measurement campaign 2). [2] Presence of fouling on sensor during inspection on 10/10/2022 (BLUE2), with copper mesh clearly missing. [3] Presence of a large crab within the sensor protection cap. [4] Significant fouling on the sensors themselves.

As an addition to point 3, it's good to point out that 'anti-fouling' may also include the actions of larger organisms like crabs. During inspection a large crab was found in each of the multisensory probes. It is not impossible that these crabs are responsible for some of the mechanical damage observed to the probes. It is for example possible that the crab is feeding on smaller organisms attaching themselves to the probes, and in trying to get a hold of them, the crab damages some of the more fragile components of the probe, such as the glass sphere and plastic protection legs of the pH sensor (Figure 10). As another example, scratch lines are clearly visible on the Chloride ISE sensor (Figure 11). The picture in Figure 10 are from the BLUE1 sensor, i.e. on the inside of the monopile. The pile itself is almost completely sealed off, except for a small opening for cables at the bottom. This means that there is very little water movement, nor any presence of floating debris in the monopile. The sensors were further more at all times covered by the protection cap. No damage from external sources can therefore occur during either operation or retrieval. This has led to the suggestion of the crab living in the sensor causing the damage.

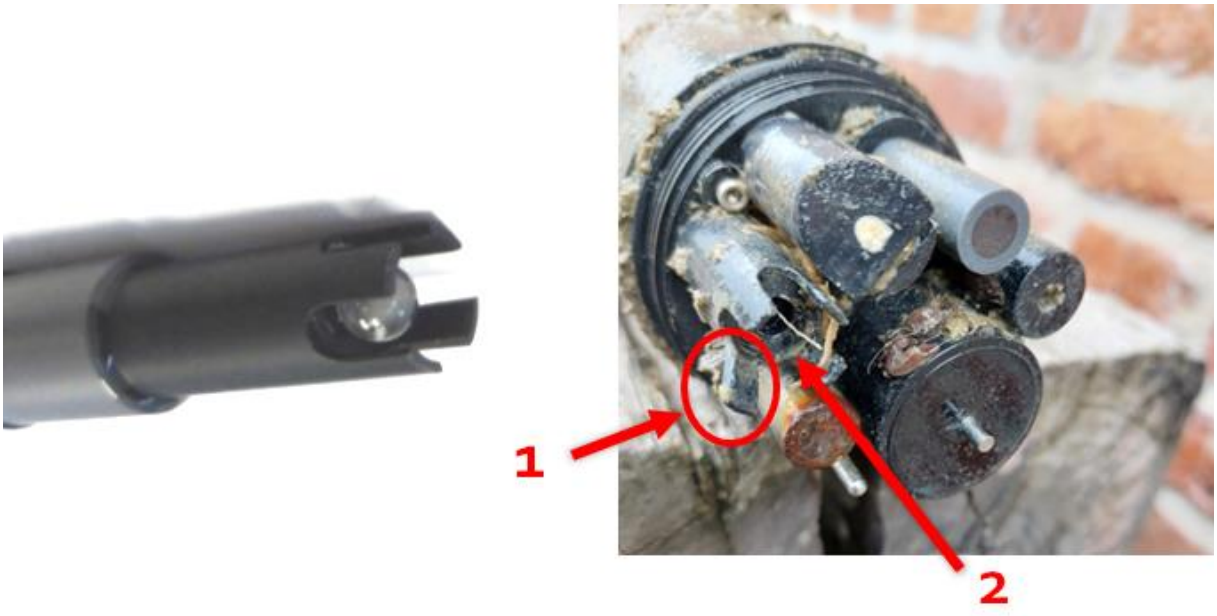

Figure 10: Left: pH probe in new condition with clearly visible glass sphere as sensor element. Right: Multisensory probe after retrieval on 10/10/2022. [1] Bent plastic protection leg. [2] Glass sphere missing.

Figure 11: Scratch marks on Chloride ISE sensor.

Analysis of the data using Python

A python script has been written for the data analysis of the sensors. The script contains the following steps:

- First the measurement files are read in python and **the data are pre-processed**. The pre-processing includes:
  - ✓ **Resampling:** In the data collection process, there were different sampling rates for the measurements initially. At the start of the project, measurements were made every minute, after approximately one month, it was decided to adjust the sampling rate, with measurements taken every half an hour. The reason for this was three-fold: (1) the rate of variation in measured parameters is slow, measuring at high frequencies therefore proved to have no added value; (2) reduce the total amount of data; and (3) be consistent with other project partners, with the decision made to have 30 min measurement intervals. For the data study, the initial measurement period is resampled at 30 minutes in the python code to have a homogeneous dataset. Resampling involves grouping the measurements based on the desired time interval (30 minutes in this case) and calculating the mean value for each group. This helps to summarize the data and provides a representative value for the specified time intervals.
  - ✓ **Removing outliers:** To ensure the quality and reliability of the measurements, a procedure for identifying and removing outliers was implemented. The identification of outliers was based on a formula that considers the median and interquartile range (IQR) of the data. A quartile is the value that marks each of the divisions that breaks a series of values into four equal parts (based on number of data points). The IQR is the range of data that captures the middle 50% of the data, excluding the lowest and highest 25%. This is a statistical measure that represents the spread or variability of a dataset. The measurement outliers are defined as those points x_i that adhere to the following formula:

    $$\boldsymbol{x_i \leq Md \pm \alpha \cdot IQR < x_i}$$

    where Md is the median and α is the significance level, which is the threshold for lower and upper boundary definition. Adjusting the value of α allows you to control the strictness of outlier identification in the boxplot method. In this case we have set the $\alpha = 3$ meaning that the threshold is three times the IQR. This means that any data points falling outside the range defined by the median plus or minus three times the IQR were considered outliers and subsequently removed from the dataset. Measurement results before and after removing the outliers are plotted in the python script.
  - ✓ **ORP:** During the first measurement campaign from 18/05/22 to 10/10/22, there was a hardware issue with the ORP sensor, resulting in a total loss of data. For the second measurement campaign from 06/02/2023-30/04/2023, the ORP sensor was replaced, providing data for the inside of the monopile. Because the SOCORRO Application and the models therein require a value for the ORP to function properly, the ORP data for the first measurement campaign was set equal to a constant value of 330mV, which is the average value observed in the second measurement campaign after an initial period of stabilisation.

- ✓ **Pressure offset**: The sensors reported a pressure value, however, after consultation with the sensor supplier it appeared that there was no pressure sensor installed in our probes. All values were therefore set to zero.

- All data are plotted in python in a single plot. The plot is implemented in such a way that the user can select which parameters are to be shown, in order to allow sufficient flexibility in having a first visual observation of the data.
- After reading and pre-processing of the data, box plots of all the measured parameters are plotted. The box plot of each parameter represents the maximum, minimum, median, first quartiles, third quartiles, upper (Q3 + (1.5 * IQR)) and lower fence (Q1 - (1.5 * IQR)). Upper and lower fences are thresholds used to identify potential outliers.
- Metal loss measurement results of Cosasco sensors and C-cube sensors are compared.
- **Corrosion rate code:** A Python code is written to calculate the corrosion rate [mm/year] based on measured metal loss [um] data obtained from Cosasco sensors. The goal is to analyse the corrosion rate over time and compare it with those measured by C-cube sensors. The advantage of corrosion rate as a measure over metal loss, is that corrosion rate (which is the first time derivate of the metal loss), gives a much stronger variability with time. This makes it much easier to visually distinguish changes in the amount of corrosion taking place as a function of time.

  The code starts by dividing the measured metal loss data into smaller ranges by means of a moving window approach. This allows for a more accurate analysis and enables tracking changes in the corrosion rate over different time intervals.

  For each window, a first order polynomial fit (a line) is applied to the data points within that window. Higher order polynomial fits have also been experimented with, however, this resulted in an overfitting of the datapoints and thereby incorrect corrosion rates. This linear fit helps approximate the relationship between the metal loss and time, allowing us to estimate the corrosion rate as an average over the window size. The slope of the line representing the polynomial fit is calculated, and this slope value corresponds to the corrosion rate for that specific window.

  The code follows a moving window approach, which means that after calculating the corrosion rate for a window centred on a certain timestamp, it moves on to the data point at the next timestamp. This sliding of the window allows for a continuous analysis of the data, capturing changes in the corrosion rate as it progresses over time.

  The user has the flexibility to select the size of the moving window and the shift between each window. For our study, a moving window of 1 day is applied, indicating that each window spans a 24-hour period 48 data points are included. The 1-day size of the window was determined after experimenting with different window sizes ranging from 6 hours to 2 days. The 1 day time window provides a good compromise between sensitivity and stability. The shift between windows is set to 30 minutes, meaning that the window slides by 30 minutes each time to analyse the next time interval. Finally, the slopes of the polynomial fits for each window, representing the corrosion rates, are stored as a separate column data, which is useful for further analysis or visualization of the data.
- **Correlation study:** Dissolved oxygen, conductivity, temperature, ORP, pH, Chloride concentration and the calculated corrosion rate for BLUE1 and BLUE2 are selected for a

correlation study. Correlation plots based on Spearman, Pearson, and Kendall methods are presented. As written earlier, observing the pair plots enables to choose the right correlation method. Having all the three methods implemented facilitate the study.

- ✓ Spearman's Rank-Order Correlation (Spearman): Spearman's method measures the strength and direction of the monotonic relationship between two variables. It calculates the correlation coefficient based on the ranks or ordinal positions of the data points. Spearman correlation is suitable for both continuous and ordinal variables. It is robust to outliers and does not assume linearity between the variables.
- ✓ Pearson's Correlation Coefficient (Pearson): Pearson's method measures the linear relationship between two continuous variables. It calculates the correlation coefficient based on the covariance and standard deviations of the variables. Pearson correlation assumes a linear relationship and normality of the variables. It is sensitive to outliers and can be influenced by extreme values.
- ✓ Kendall's Rank Correlation (Kendall): Kendall's method measures the strength and direction of the rank correlation between two variables. It calculates the correlation coefficient based on the number of concordant and discordant pairs in the data. Kendall correlation is suitable for both continuous and ordinal variables. It is non-parametric, meaning it does not assume a specific distribution or relationship between the variables. Kendall correlation is robust to outliers and works well with small sample sizes.

In summary, Spearman correlation focuses on the rank or ordinal relationship, Pearson correlation measures the linear relationship between continuous variables, and Kendall correlation evaluates the rank correlation without assumptions about distribution or linearity.

- Comparison between BLUE1 and BLUE2 measured parameters with pair plots (one parameter plotted against the other, without time axis), either similar or various y-axis. This enables to study the variation of the measured parameters during the measurement period. Pair plots help to understand correlation between the parameters.
- In addition to pair plots, a code is also implemented to plot 2 different parameters as a function of time, with each parameter having a separate y-axis. This again allows to further study the correlation between two individual parameters. The selection of which parameters to study can be based on the correlation study.
- The format of the data files is adapted so that it has the correct format to be uploaded in the SOCORRO Application.
- The format of the pre-processed data as well as the output from the SOCORRO App models, is later adjusted according to that of the e-BO Offshare® platform and the data are uploaded.

Results and Conclusions

Corrosion data

Corrosion data is collected at the Blue Accelerator in three different ways: using Electrical Resistance Probes from COSASCO, using sensors from C-Cube (potentiodynamic measurements) and using steel coupons (mass loss).

The primary output from COSASCO Electrical Resistance probes is a measure of the electrical resistance over a very thin corroding coupon. The electrical resistance is used to calculate a metal loss in micrometer. This is done in the data acquisition unit from COSASCO. The result is transmitted as an analogue signal (4-20mA), which then needs to be transformed back in a mass loss by the user (here Sirris) according to a function provided by COSASCO. The slope of the metal loss with respect to time gives the corrosion rate. An algorithm was implemented in python to calculate the corrosion rate.
In order to be able to calculate the corrosion rate, the data first needed to be resampled. In the beginning of the monitoring campaign, the data was recorded every minute. As such a high sampling frequency doesn't add value for a relatively slowly changing process such as corrosion, the sampling frequency was later reduced to once every 30min. To have a stable corrosion rate calculation, a data frame with constant time between data points is required, hence the need for resampling.
From the resampled data, the corrosion rate was calculated using a moving window with a step size of 30min. This means that for every data point in the original data series, a corrosion rate is calculated. The window starts at halve the window length before the data point for which the corrosion rate is calculated, and ends at halve the window length beyond it. The corrosion rate within this window is calculated by fitting a straight line to the metal loss within this window, with the slope of the line being the corrosion rate. Finally, a factor correction is applied to change into units of mm/yr.
The optimal window size was determined iteratively. With a too short window size, the corrosion rate calculation is unstable and results in large variations due to fluctuations in the raw data. With a too large window size, the short term natural variations in corrosion rate are lost. Two days was found to be a good compromise in terms of window size.
From the C-Cube probes, corrosion rate is the primary output. By integrating corrosion rate over time, metal loss can be obtained. Both outputs are provided by C-Cube.
The corrosion rate and metal loss for both the internal (BLUE1) and external (BLUE2) corrosion are given in the figures below.

From the COSASCO data in Figure 12 and Figure 13 it can be seen that the initial corrosion rate is high, followed by a gradual decrease in the corrosion rate. This can be related to the build up of a corrosion product layer on the sensor coupons, which reduces the accessibility to oxygen. Starting from September a second decline in the corrosion rate can be observed for BLUE1, this is probably linked to decreasing water temperatures. During the summer period an average corrosion rate of approximately 0.1mm/yr is obtained using the COSASCO probes. During the winter period the corrosion rate drops to approximately 0.025-0.030 mm/yr.
For BLUE2, a sudden increase in the corrosion rate is observed on 1 August 2022. At that time, maintenance of environmental sensors is undertaken. During the maintenance, the corrosion probes were above water for a period of 2 days. It is believed that this has caused the increase in corrosion rate by a change in the corrosion mechanism. The hypothesis is that micro and macro biological live died off during the 2 days above water, with break-down products possibly acidifying the local environment and breaking down the formed corrosion product barrier. Upon re-submersion in water, the corrosion process would again start at a higher rate, until a new corrosion product barrier is formed and a new equilibrium is established. The measured 'stabilised' corrosion rates are in the range of 0.1

to 0.15 mm/yr. The variability in the data makes it difficult to establish a clear distinction between corrosion rate during summer and winter periods.

From the graphs, it can clearly be seen that the corrosion rates as measured using the C-Cube sensor are significantly higher than the corrosion rates from the COSASCO sensor. By comparing to the results from mass loss coupons, it can be concluded that the C-Cube sensor is overestimating the corrosion rates, especially for the internal corrosion. The coupons were installed on 17/05/2022, at the same time of the COSASCO and C-Cube sensors. Coupons from the outside of the monopile were retrieved on 10/10/2022 and coupons from the inside of the monopile on 25/01/2023. The corrosion rate was determined from mass loss measurements and are shown in Table 1. Three coupons were measured for BLUE2, two coupons for BLUE1. For comparison, the corrosion rate calculated based on the mass loss given by the COSASCO probes on the same day is given. The corrosion rates from the mass loss coupons are in line with the corrosion rates from the COSASCO probes, although the COSASCO probes are somewhat underestimating the corrosion rate.

Location	Installation	Retrieval	Exposure time	Corr. Rate	COSASCO Av.
External (BLUE2)	17/05/2022	10/10/2022	147 days	0.35 mm/yr	0.28 mm/yr
Internal (BLUE1)	17/05/2022	25/01/2023	254 days	0.16 mm/yr	0.09 mm/yr

Table 1: Corrosion rates obtained from mass loss coupons, and comparison to COSASCO corrosion rate.

Figure 12: BLUE1 – Corrosion rate

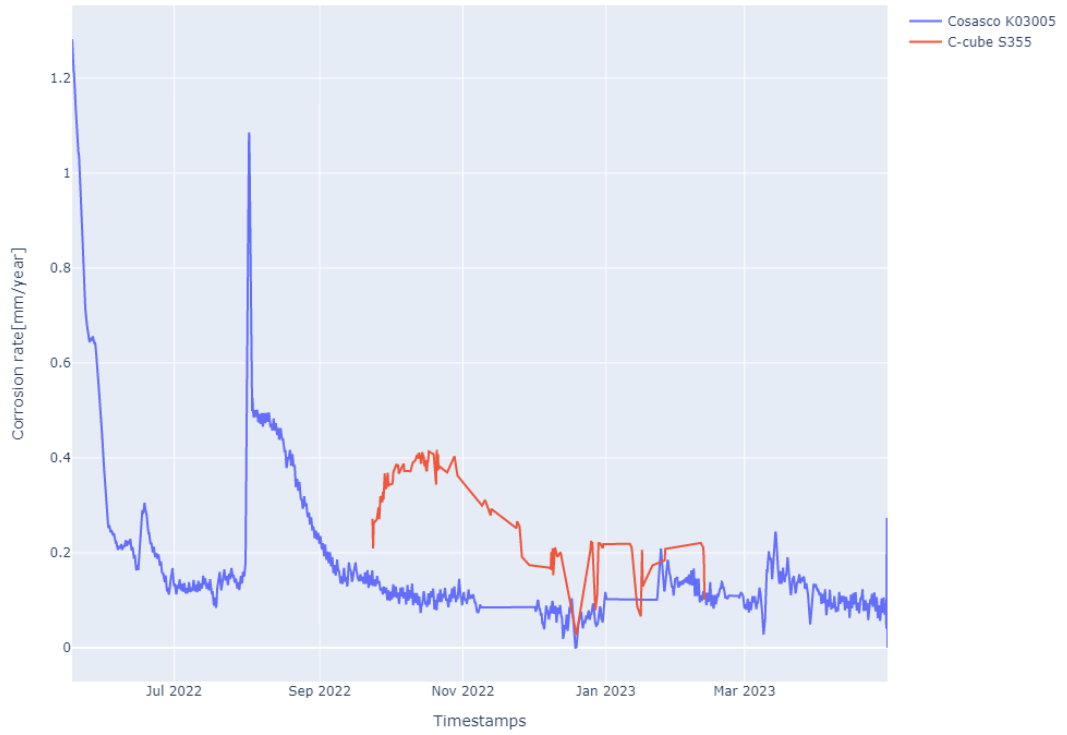

Figure 13: BLUE2 – Corrosion rate

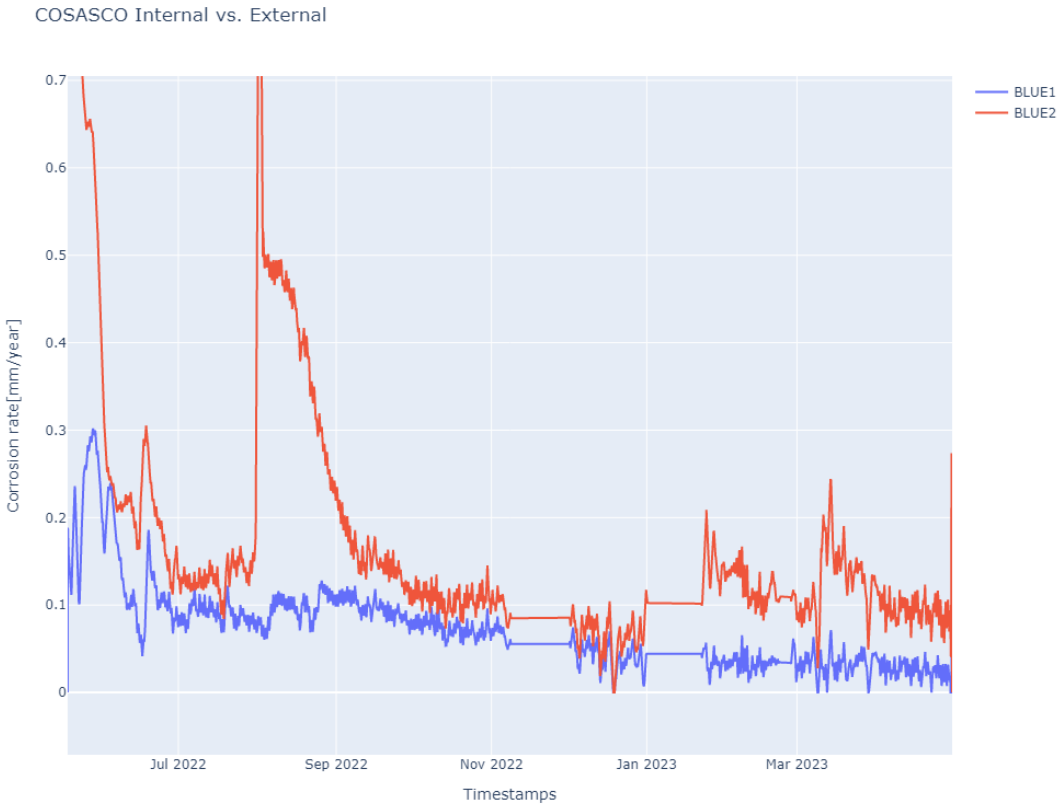

Figure 14: COSASCO corrosion rates. Internal (BLUE1) vs. external (BLUE2) corrosion.

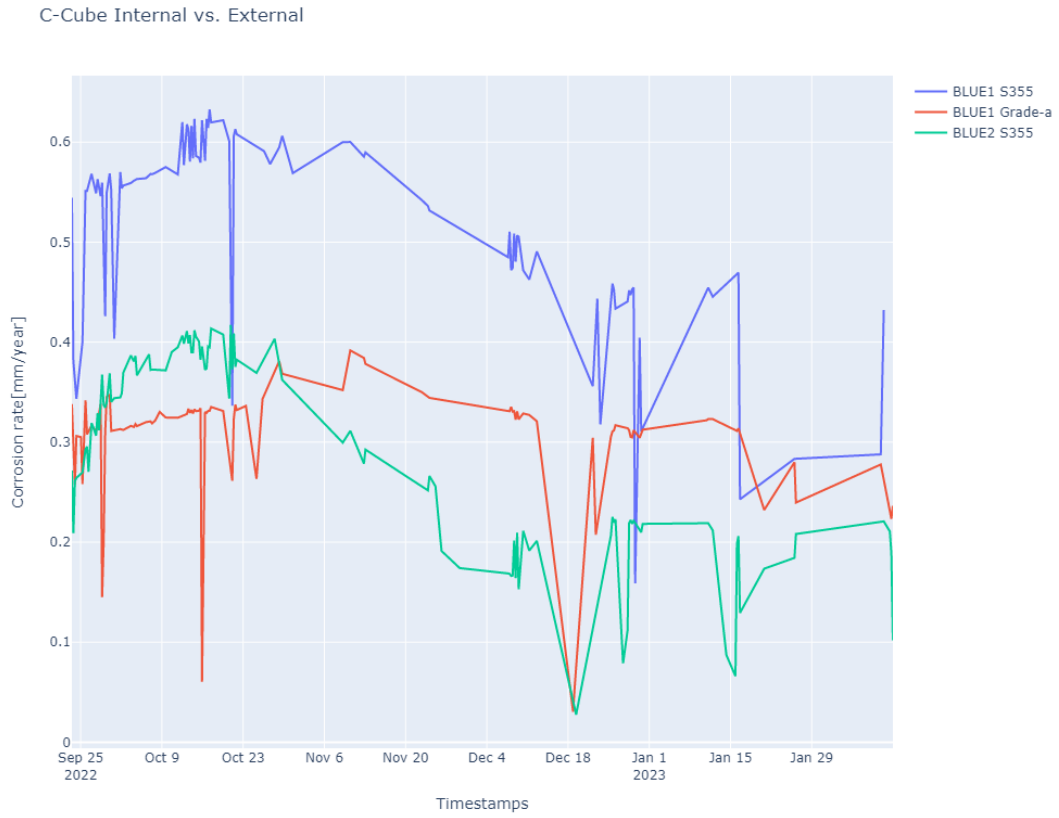

Figure 15: C-Cube corrosion rates. Internal (BLUE1) vs. external (BLUE2) corrosion.

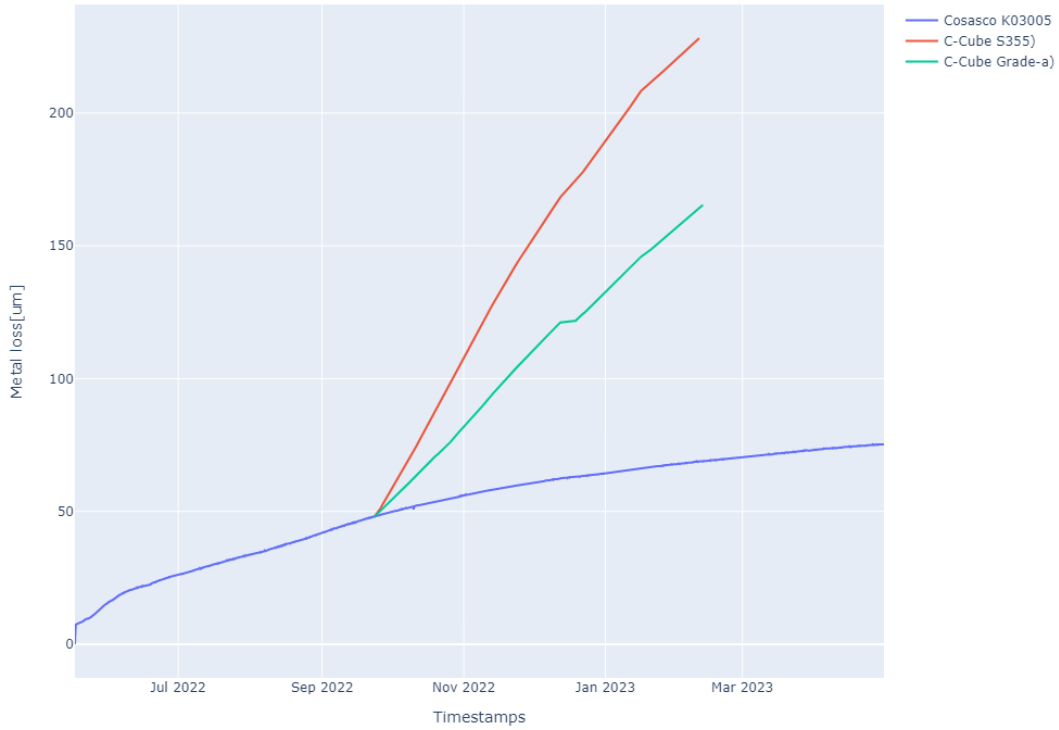

Figure 16: BLUE1 – Metal loss

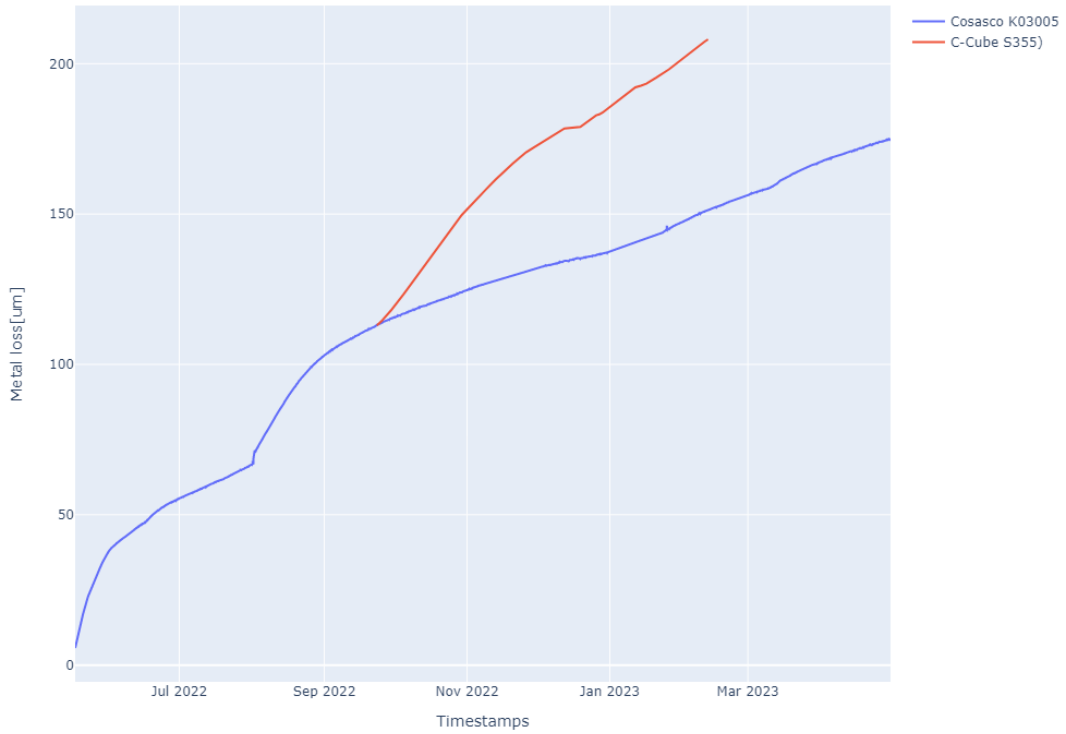

Figure 17: BLUE2 – Metal loss

For the graphs of metal loss, it should be remarked that no reliable data from the C-Cube sensors was available before 23/09/2022 due to a sensor malfunction. The metal loss has therefore been drawn as is starting from the same level as the COSASCO metal loss on 23/09/2022 to allow for easier comparison.

The discrepancy between the COSASCO and C-Cube sensors is believed to be due to the specific design of the electrodes in the C-Cube sensor. Measurements at the Blue Accelerator are planned to be continued and Sirris is currently working with C-Cube on an updated design of the sensor that should allow to match measured corrosion rates better with the results from mass loss coupons.

The corrosion coupons from external exposure exhibit a much more pronounced pitting profile than the internal coupons, as can be seen from Figure 18 and Figure 19. In addition, the amount and type of fouling found on internal and external coupons is different. The fouling layer on external coupons is not only thicker, it also contains more macro-organisms, i.e. larger organisms like mussels, types of worms, etc. The difference in fouling is illustrated in Figure 20.

When comparing corrosion rates between BLUE1 (internal corrosion) and BLUE2 (external corrosion), it becomes clear that the corrosion inside the monopile is proceeding at a significantly slower rate. This will be discussed in more detail in the next paragraphs.

Figure 18: Left: coupons exposed on the outside of the monopile for 147 days. Right: coupons exposed on the inside of the monopile for 254 days.

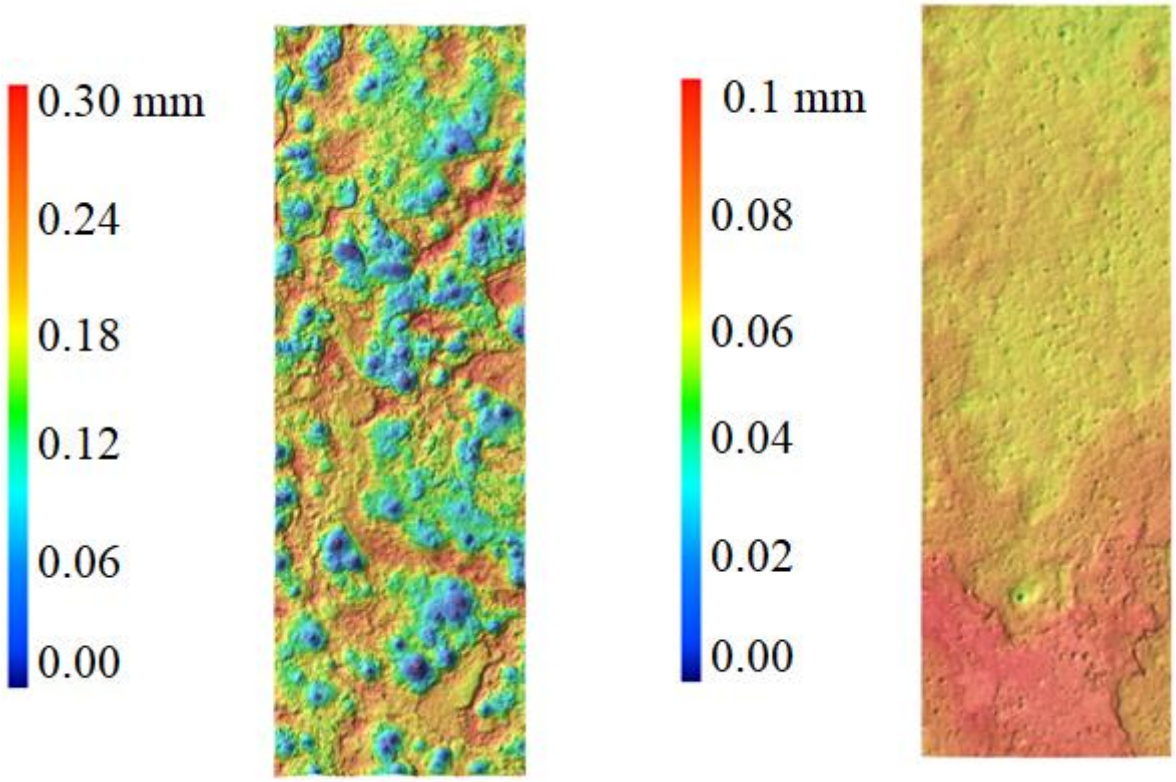

Figure 19: Left: 3D scan of coupons exposed on the outside of the monopile for 147 days. Right: 3Ds can of coupons exposed on the inside of the monopile for 254 days.

Figure 20: Illustration of fouling on corrosion coupons. Left: external; Right: Internal.

Measurement campaign 1: 18/05/2022-10/10/2022

Introduction

Corrosion rate sensors do not require maintenance and can remain operational for years without manual intervention. From the point of view of maintenance and calibration of sensors, monitoring of water quality parameters is much more difficult, as has already been pointed out under the paragraph 'Timeline and technical remarks'. The measurement data itself also shows this. The multiprobes used for measurement of the water parameters needed to undergo extensive maintenance and were removed from the demo site on October 10th 2022, therefore ending the first measurement campaign. After 10/10/2022, corrosion data was still collected, but no environmental parameters, until the start of the 2nd measurement campaign.

While the sensors and corrosion coupons were already installed at the demo site on 17/05/2022, we chose to let the measurement campaign officially start on 18/05 because some start-up phenomena caused a number of anomalous readings during the day of installation. Measurement campaign 1 can further be split in three time periods:

- 18/05/2022 till 16/07/2022: Good data for both the internal (BLUE1) and external (BLUE2) sensor setups. Starting from 16/07 the Dissolved Oxygen sensor on BLUE2 gave anomalous readings, with also Conductivity and pH starting to give diverting sensor readings.
- 16/07/2022 to 25/08/2022: Good data for the internal (BLUE1) sensor setup. Starting from 25/08 the pH reading of BLUE1 suddenly drops to an unrealistically low value, without a corresponding change in any of the other values being measured.
- 25/08/2022 to 10/10/2022: Fairly good data for the internal (BLUE1) sensor setup, except for pH.

Overview of measured data

An overview of all measured data in Figure 21 and Figure 22. For BLUE1, the data is shown until 25/8/2022, for BLUE2, the data is shown until 16/07/2022. Later data did not have good measurements for all the parameters needed to analyse the data with the SOCORRO application, nor did it yield additional insights on correlations between parameters. The later data is therefore not shown here.
Boxplots of the data in the same time windows is shown in Figure 23 and Figure 24.
Summarizing the baseline situation, the following are 'expected' values and variations for the measured parameters:

- Temperature: 11+/-9°C
- EC: Measurements in the Belgian North Sea give 30-47 PSU.
- DO: Saturation should be around 100%
- pH: 8.1-8.2

Looking at the boxplots for BLUE1 and BLUE2, a few observations can already be made.

- Temperature: Relatively high for both BLUE1 and BLUE2. This is because measurements are made during the summer period.
- EC: BLUE1: very small variation; BLUE2: normal value and variation
- DO: BLUE2 indeed around 100% and smaller variation than BLUE1, BLUE1, much lower and much higher variation

- pH: normal value and variation for both BLUE1 and BLUE2, note difference in scale for BLUE1 due to a few outliers

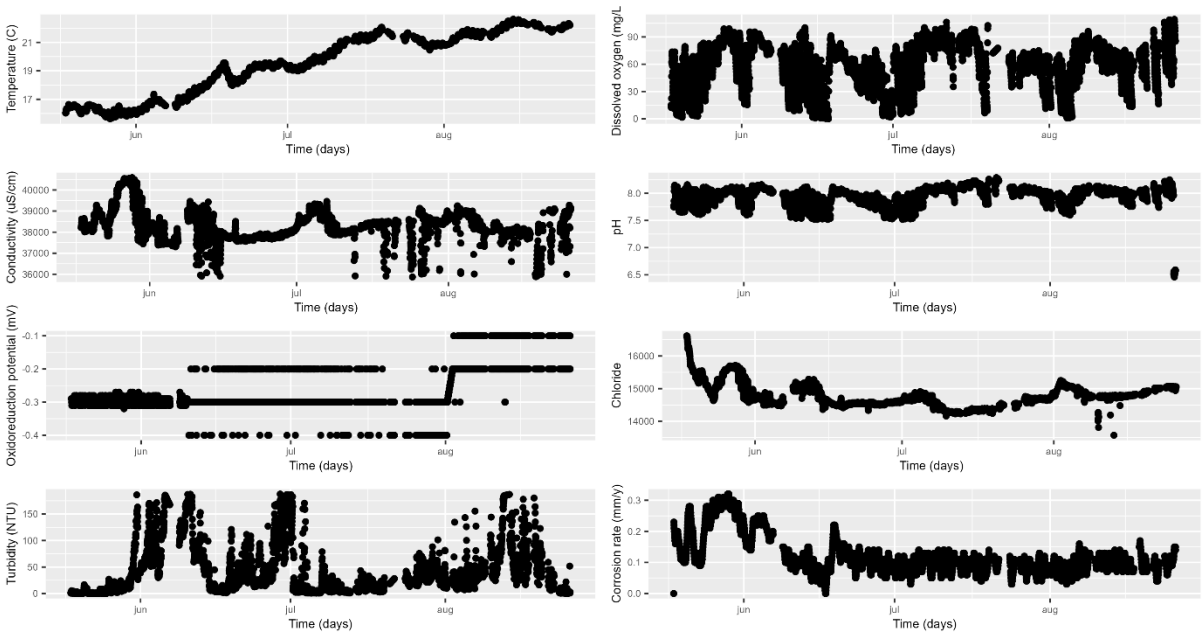

Figure 21: Timeseries of measured parameters at the Blue Accelerator, location BLUE1 (i.e. inside of the monopile). Data is shown from 18/05/2022 till 25/08/2022.

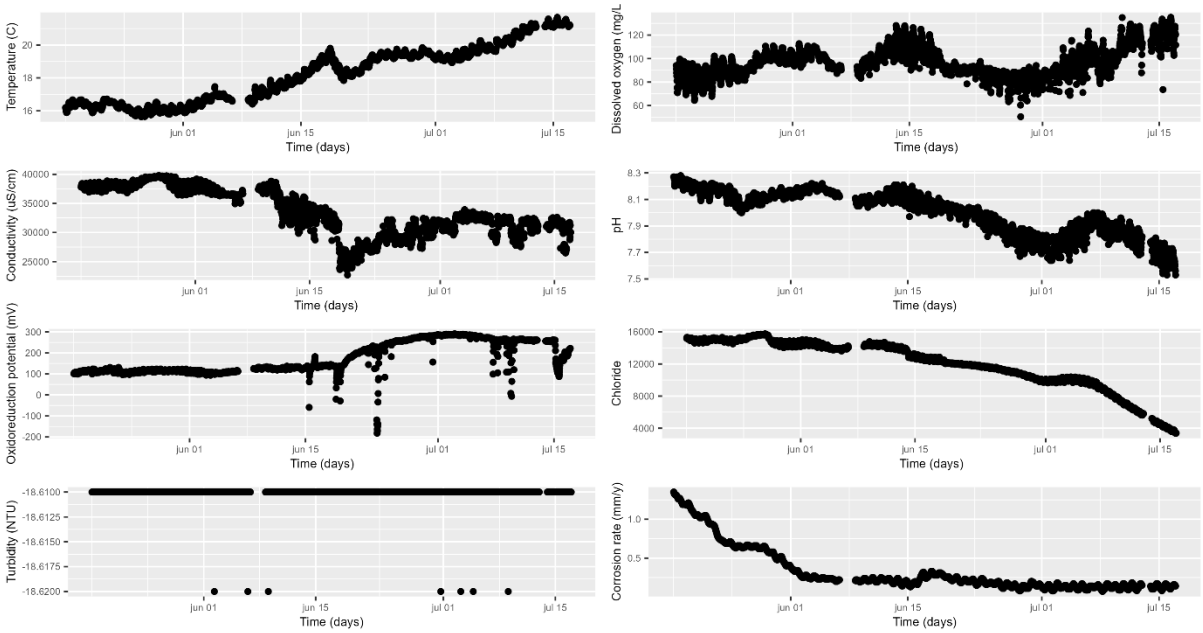

Figure 22: Timeseries of measured parameters at the Blue Accelerator, location BLUE2 (i.e. outside of the monopile). Data is shown from 18/05/2022 till 16/07/2022.

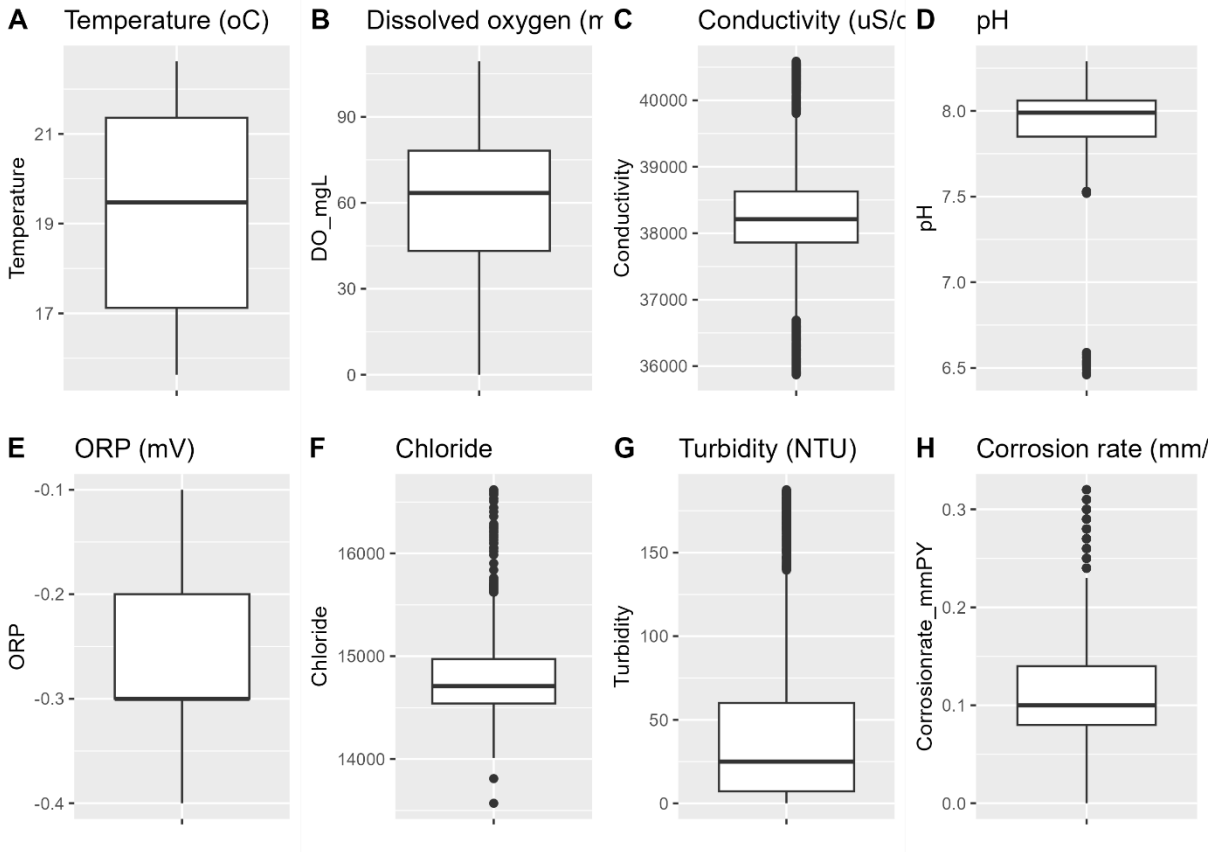

Figure 23: Boxplots of measured parameters at the Blue Accelerator, location BLUE1 (i.e. inside of the monopile). Data is shown from 18/05/2022 till 25/08/2022.

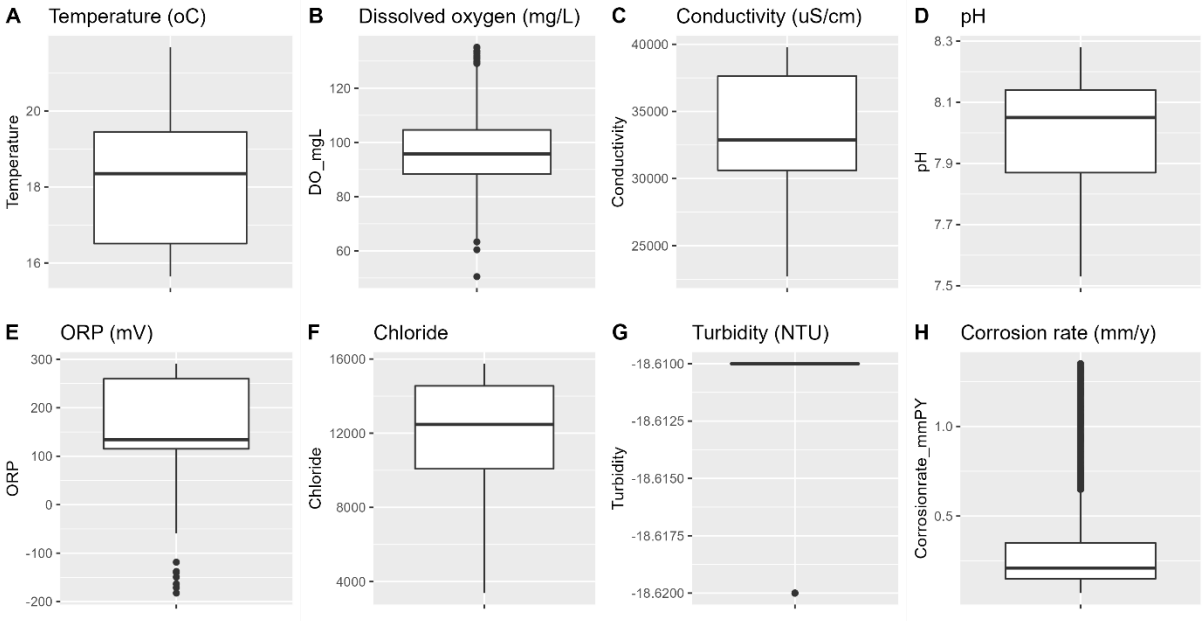

Figure 24: Boxplots of measured parameters at the Blue Accelerator, location BLUE2 (i.e. outside of the monopile). Data is shown from 18/05/2022 till 16/07/2022.

A high level comparison between BLUE1 (internal) and BLUE2 (external) can be made by looking at the averages of the measured data over a certain time period. Averaged data is shown in Table 2. The parameters with the largest variation between BLUE1 and BLUE2 are highlighted (bold, underlined).

	BLUE1	BLUE1	BLUE2
Start-end date for average	18/05/22-16/07/22	18/05/22-25/08/22	18/05/22-16/07/22
Material	S355	S355	S355
CorrRate (Cosasco) [mm/yr]	0.14	0.12	0.34
CorrRate (Coupon) [mm/yr]	**0.16**	**0.16**	**0.35**
Date of coupon retrieval	25/01/2023	25/01/2023	10/10/2022
Temperature	18.18	19.55	18.2
Dissolved Oxygen [mg/l]	**4.65**	**4.64**	**7.85**
Dissolved Oxygen [%]	**58.64**	**59.94**	**97.15**
Conductivity [µS/cm]	38285.88	38264.51	33655.19
pH	7.92	7.96	8.01
pH [mV]	-58.06	-60.16	-62.08
Chloride [ppm]	14758.69	14756.4	11923.29
Turbidity [NTU]	45.08	44.83	-18.61

Table 2: Averaged data for Measurement Campaign 1. BLUE1 = inside the monopile. BLUE2 = outside the monopile.

Correlation between water parameters

An overview of pair-wise correlation factors and plots is given for BLUE1 in Figure 25 and for BLUE2 in Figure 26. Correlation factors are calculated according to Pearson.

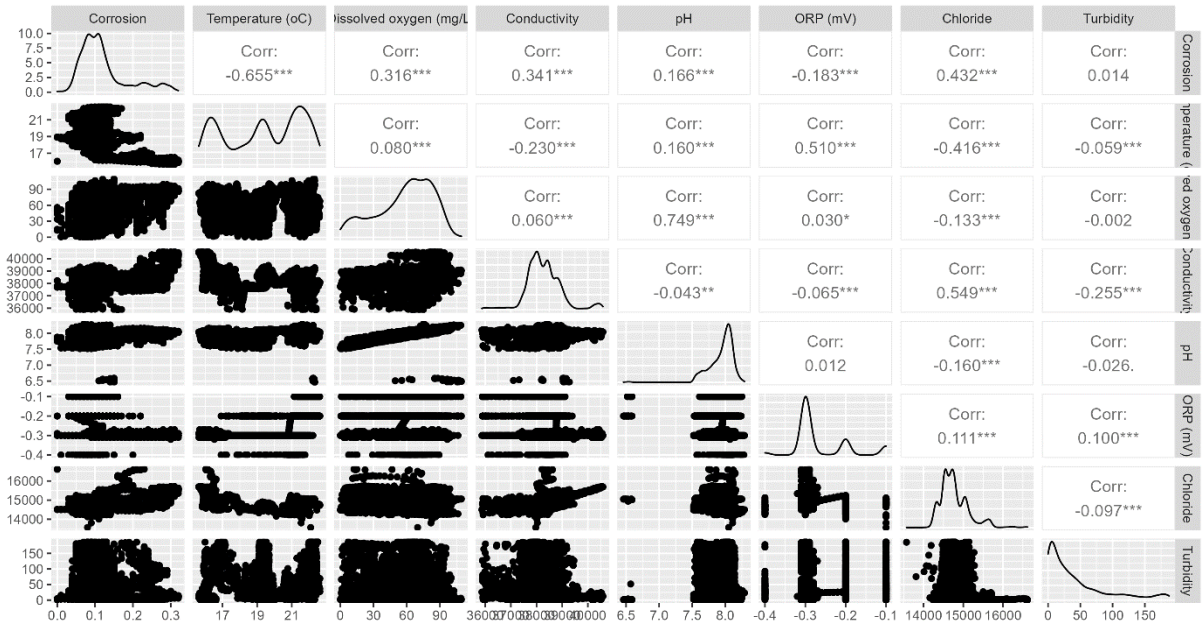

Figure 25: Pair-wise correlation factors and plots for BLUE1. Calculation for correlation factors according to Pearson.

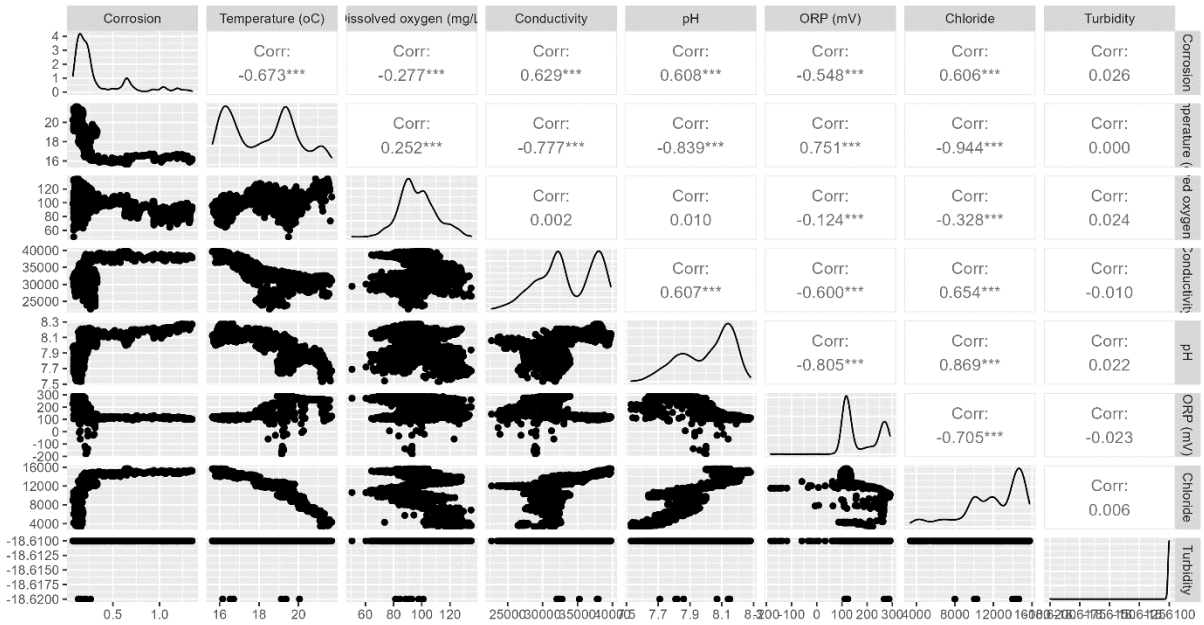

Figure 26: Pair-wise correlation factors and plots for BLUE1. Calculation for correlation factors according to Pearson.

DO vs. pH

From the plots and correlation factors, it can be seen that there is one very high correlation factor, namely between Dissolved Oxygen and pH for BLUE1. The pair plots in Figure 27 clearly demonstrate this correlation for the inside of the monopile (BLUE1), while it is entirely absent for the outside of the monopile (BLUE2). In addition Figure 28 shows that both DO and pH exhibit 12 hour cycles at BLUE1. Taking the data of July 3rd and 4th as an example, it can be seen from Figure 29 that the changes in DO follow the same periodicity as the changes in tidal level. The observed 12 hour cycles in DO and pH are therefore most likely linked to the tidal cycles. A possible explanation is given below. The synchronisation is not perfect. Why the DO is not perfectly synchronised with tidal levels is not yet understood and requires further study.

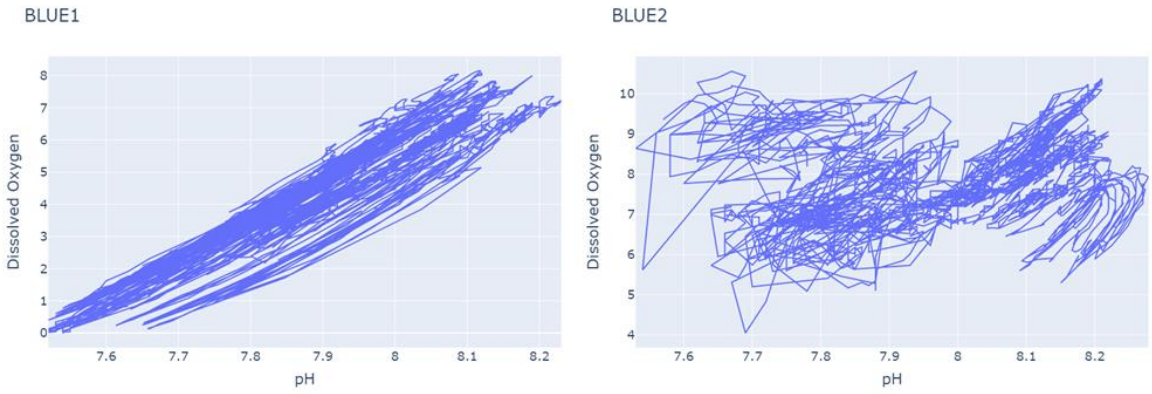

Figure 27: Pair plots of DO vs. pH for BLUE1 and BLUE2 in the period 18/05/2022 to 16/07/2022.

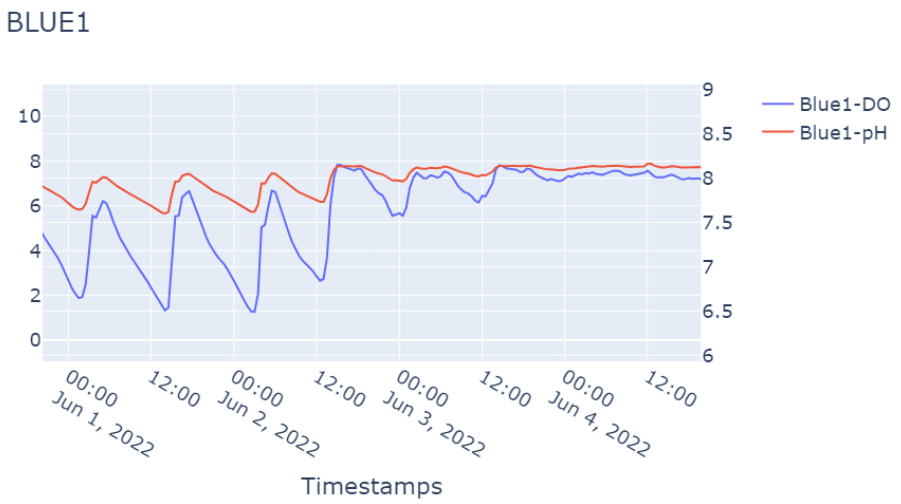

Figure 28: Illustration of synchronised 12h cycles in DO and pH measurements at the inside of the monopile (BLUE1). (Left y-axis: DO in mg/l; Right y-axis: pH)

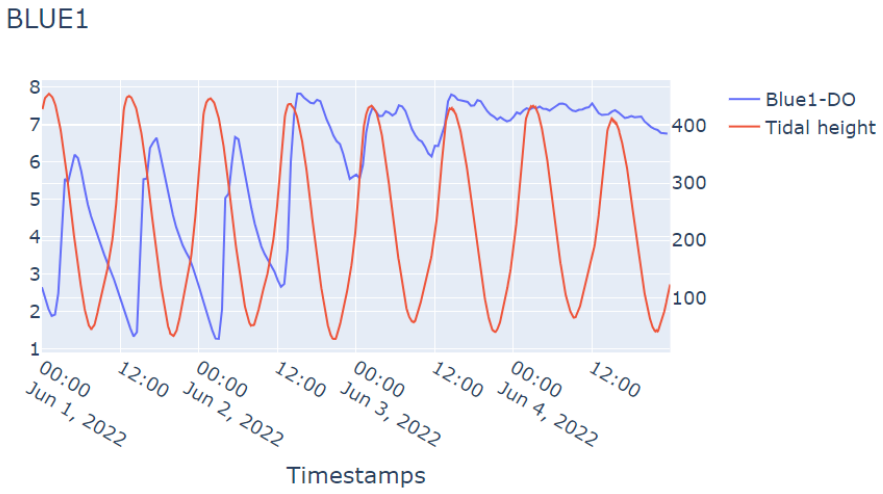

Figure 29: DO (blue) and tidal height (red) for BLUE1. Illustrating the similar periodicity for both. (Left y-axis: DO in mg/l; Right y-axis, tidal height in cm).

The observed correlation and cycles can be understood from the design of the monopile, which has a single, small opening near the seabed. The water inside the monopile is therefore not easily mixed with the seawater on the outside. This can already be seen from the difference in dissolved oxygen, which is much lower inside the monopile than on the outside (see Table 2). It can be understood that the water inside the monopile is partly refreshed with every tidal cycle. When the tide is falling, the water level outside the monopile reduces. As the monopile and the sea around it are working communicating vessels, water will start flowing out of the monopile. When the tide is rising, the water level outside the monopile increases, and water will start flowing into the monopile. This means that a certain percentage of the water inside the monopile is refreshed, with the percentage being proportional to the tidal difference of the tidal cycle.

On June 3rd and 4th, the variations in DO with tidal cycles become much less pronounced. A possible explanation for this is given in Figure 30. It can be seen that the variation in DO levels reduces with

increasing wave height. As the wave height increases (relative to the tidal level differences), the amount of water refreshment due to waves passing is also increased. As the wave heights become sufficiently large, water is sufficiently mixed and refreshed in order to prevent a drop in DO.

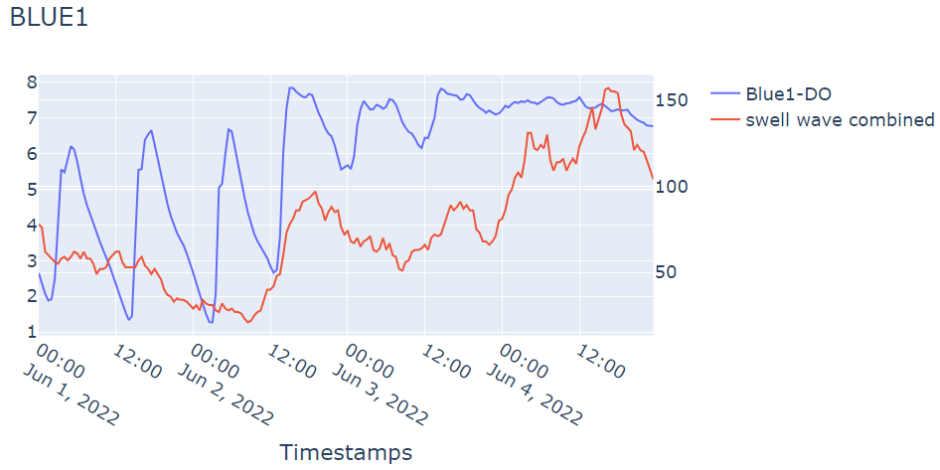

Figure 30: DO (blue) and combined wave and swell height (red) for BLUE1. Illustrating thar the variation in DO reduces with increasing wave height. (Left y-axis: DO in mg/l; Right y-axis, wave height in cm).

The pH and DO inside the monopile are lower than that on the outside of the monopile, as can be seen in Figure 31 and Figure 32. The difference at the time of low tide is higher than the average difference given in Table 2. As a result, when the tide starts to rise, water with a higher DO and higher pH is flowing into the monopile, resulting in an increase in DO and pH levels. In the time between high tide and low tide, no new water flows into the monopile. During that time, oxygen is consumed by the organisms living inside the monopile. At the same time, bacterial live likely produces acidic substances, resulting in the observed drop in pH.

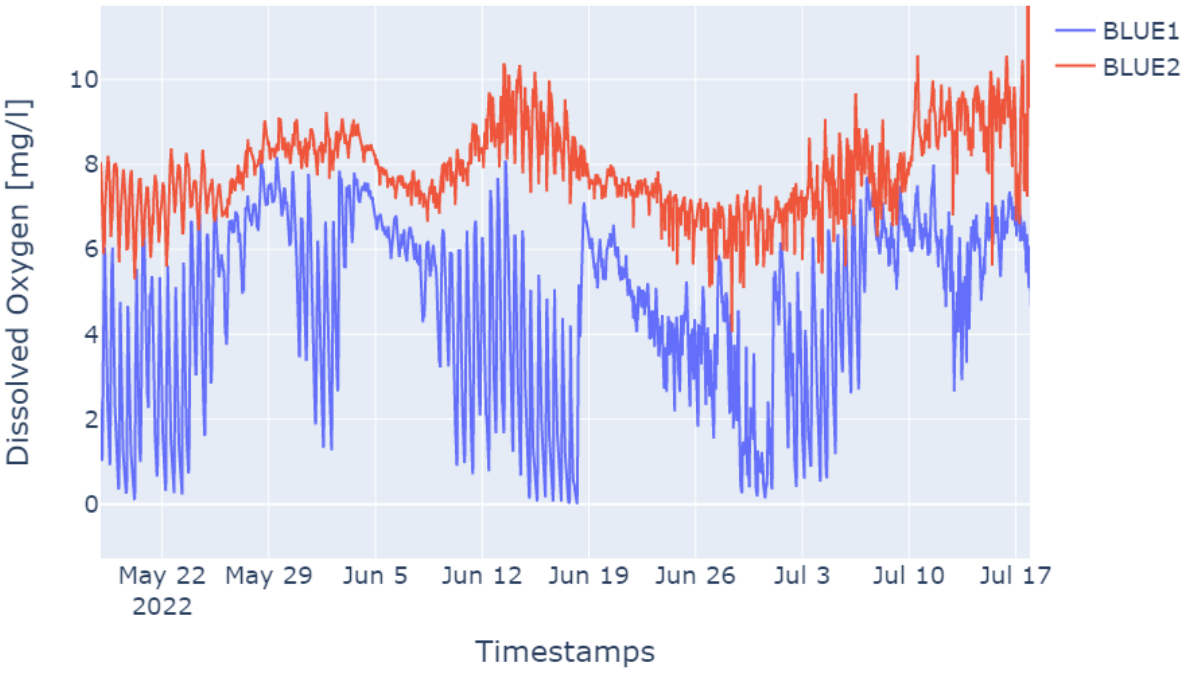

Figure 31: Time plots of Dissolved Oxygen for BLUE1 (internal) and BLUE2 (external).

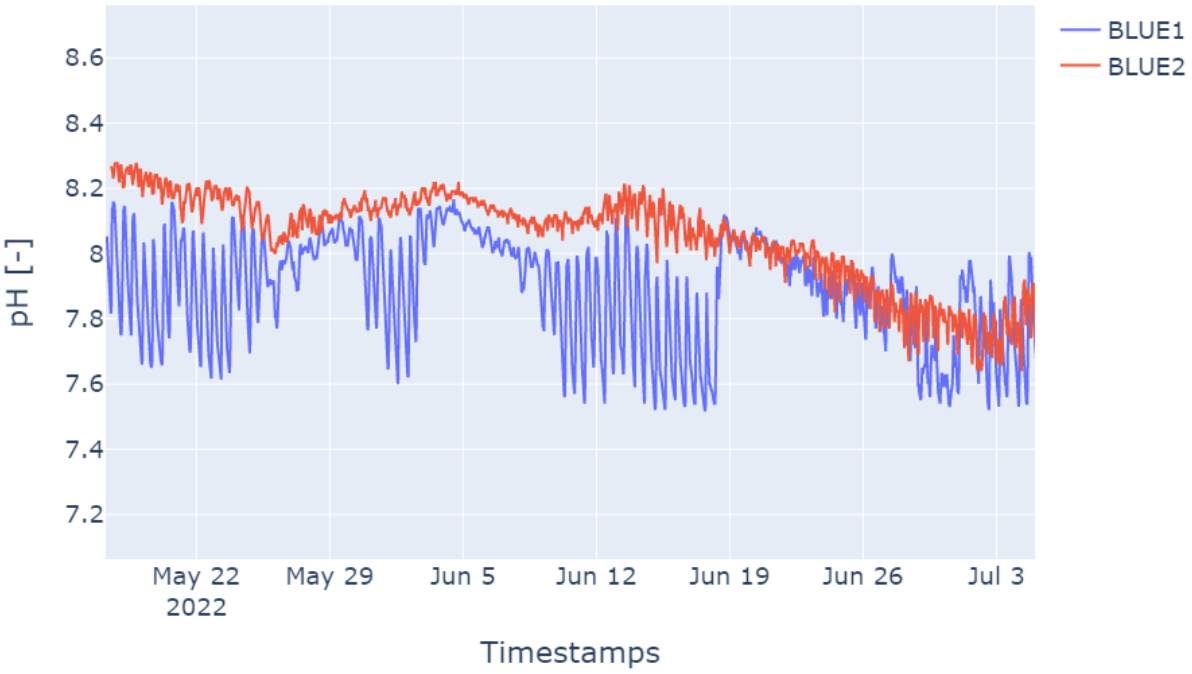

Figure 32: Time plots of pH for BLUE1 (internal) and BLUE2 (external).

Temperature and conductivity

A correlation between temperature and conductivity can be expected. Conductivity increases with increasing temperature if other parameters remain unchanged. In BLUE1 (internal) a linear correlation between temperature and conductivity can indeed be seen in the pair plot in Figure 33. Super imposed on the linear correlation are other variations in conductivity which may to a large extent be due to noisy data. In BLUE2, the expected correlation cannot be observed. However, when looking at the conductivity data, it is clear that there is a decreasing trend which is not in line with the expectations and to much lower values than what can be expected of seawater. This reflects a strong likelihood of sensor failure, and the data has therefore not been subject to further study.

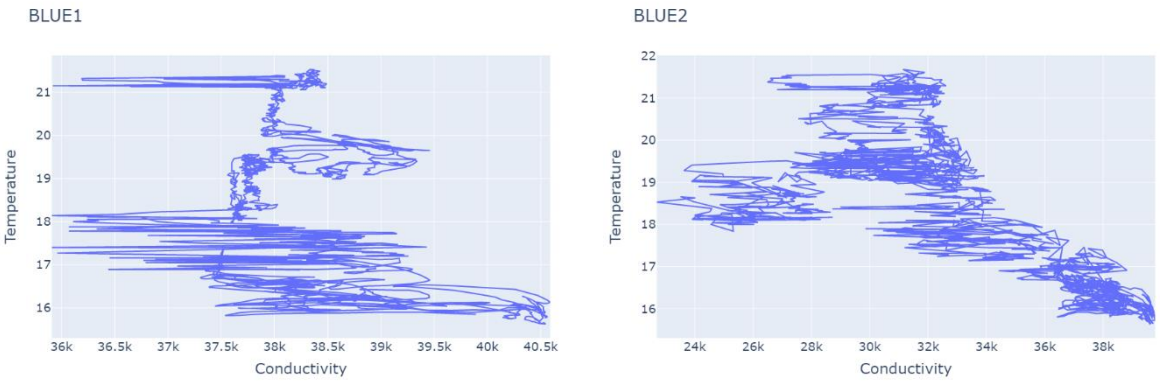

Figure 33: Pair plots for temperature (in °C) against conductivity (in µS/cm) for BLUE (left) and BLUE2 (right). Data from the beginning of the measurement campaign to 16-07-2022.

Chloride ion concentration and conductivity

A higher chloride ion concentration is expected to result in a higher conductivity. The pair plots in Figure 34 show that this correlation is indeed observed. Unfortunately, especially for BLUE2, from 05-06-22 onwards the conductivity data becomes unreliable. Therefore the pair plots have been limited to include only the data up to this date.

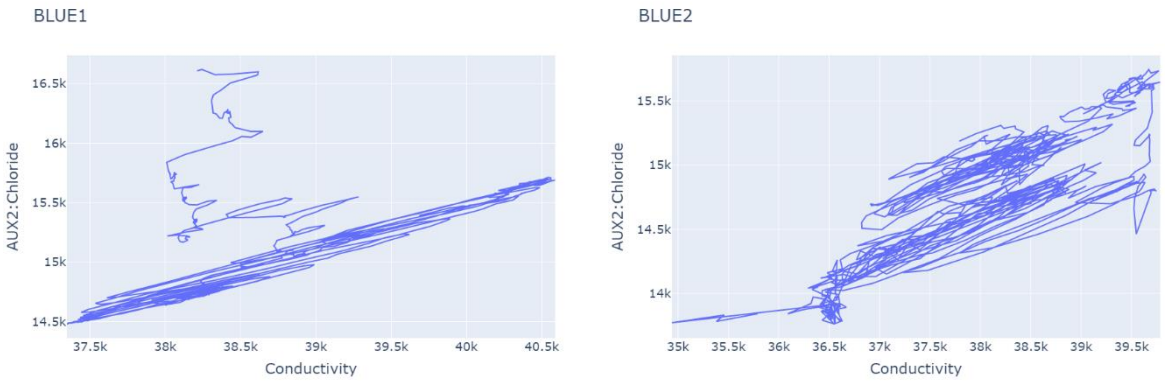

Figure 34: Pair plots for Chloride ion concentration (in ppm) against conductivity (in µS/cm) for BLUE (left) and BLUE2 (right). Data from the beginning of the measurement campaign to 05-06-2022.

Dissolved Oxygen and temperature

The oxygen saturation concentration in water is temperature dependent, with higher water temperatures resulting in lower saturation concentrations. In the current measurement campaign, no correlation between DO and temperature could be discerned. For the inside of the monopile (BLUE1) this can be understood from the strong correlation between DO and the tidal levels overshadowing the correlation with temperature. Also on the outside of the monopile (BLUE2) such correlation is not observed, although temperature are increasing from 5°C to 20°C during the period of reliable DO measurements. A timeseries plot of both DO and temperature for BLUE2 is shown in Figure 35.

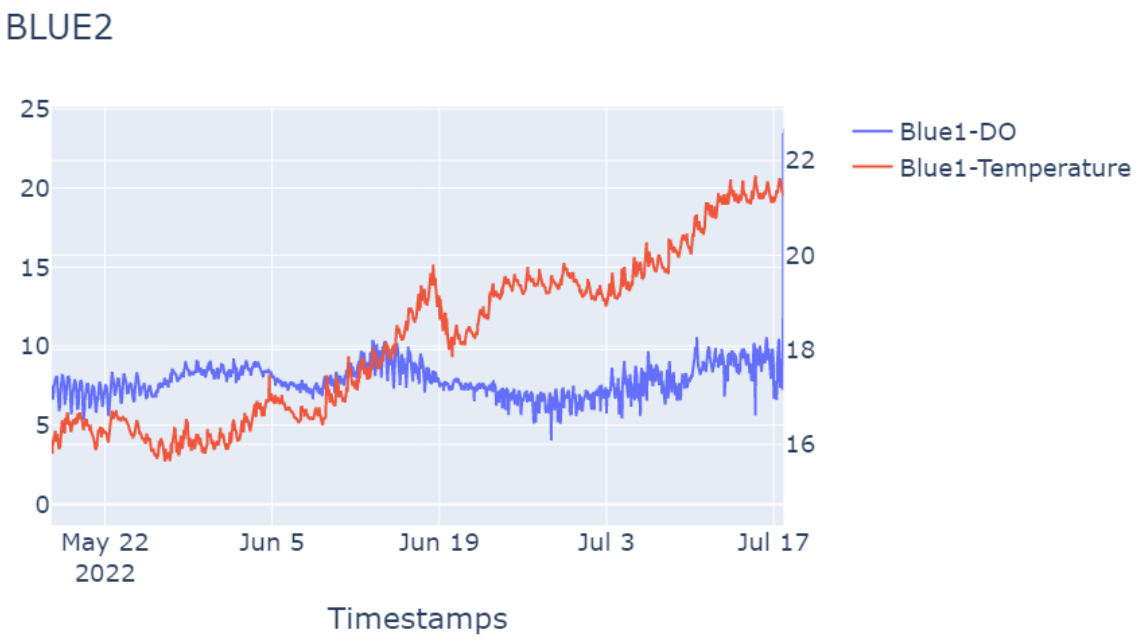

Figure 35: Timeseries plot for DO (left y-axis, mg/l) and temperature (right y-axis, °C) for BLUE2.

Correlation between water parameters and corrosion rate (BLUE1 vs. BLUE2)

From the data in Table 1, as well Figure 14, it is clear that the corrosion rate on the inside of the monopile is considerably lower than the corrosion rate on the outside of the monopile. This is confirmed by both the COSASCO sensors and the corrosion coupons.

When looking at the environmental parameters, there is one parameter that is reliably measured and shows a clear difference between BLUE1 and BLUE2: Dissolved Oxygen. The oxygen content on the inside of the monopile is much lower than on the outside, which correlates perfectly with observed corrosion rates.

Other correlations with environmental parameters could not be found.

One other remarkable difference between the internal and external samples is the amount of fouling found on the sensors and coupons. There is a much thicker layer of biological growth on the external surfaces, which also appears to consist of different types of organisms. The generation of a different micro climate below a thicker and different layer of biological growht may also play a role in the observed differences, leading to much more pronounced pitting corrosion on the outside of the monopile, with multiple pits clearly coalessing into larger 'pitted areas' (see Figure 18 and Figure 19).

SOCORRO app data analysis

The data from Measurement campaign 1 has been analysed using the SOCORRO Application. I.e. the corrosion risk has been calculated based on the available data on environmental parameters.

BLUE1

- Lab Trained: start: 0.23-0.25, in July going to 0.33, end of July again to 0.23, august 0.3-0.33

- Field Trained: start: 0.1, in July one peak to 0.15, but much smaller in width as compared to lab trained (but same time window), end of July again to 0.1, august, going to 0.15
- Overall, lab and field trained follow the same trends, but at different absolute value and higher level corrosion risks are over shorter time periods in the field trained model.

BLUE2

- Lab Trained: start: 0.25, than 0.235, at the end, peaks going to 0.30
- Field Trained: start: 0.1, than 0.096, at the end, peaks going to 0.11
- Overall, lab and field trained follow the same trends, but at a different absolute value

The general conclusion from this is that the lab trained model results in corrosion risks which are a factor 2-3 higher than then field trained model. This most likely is a result of the corrosion rates in the training dataset being higher for the lab data than the field data. However, the general trend is comparable. ***This illustrates that the approach followed by SOCORRO to report a risk rather than an absolute value of corrosion rate makes sense, as the absolute value is very difficult to predict accurately, however it is possible to predict relative differences in exposure risk.***

Another conclusion is that the corrosion rate for BLUE1 is slightly higher than for BLUE2 when averaged over the entire period. This is also clear from the accumulated corrosion risks (not shown here). This does not agree with the experimental observations, which show that the corrosion rate for BLUE2 is twice that for BLUE1. The main reason for the difference in corrosion rate is a different dissolved oxygen content. It should be notes that in the Field data set, there were only very small differences in dissolved oxygen content in the training data set. Similarly, the lab data set also contained only very limited data points for different oxygen content. As such, it is not surprising that the difference between BLUE1 and BLUE2 is not captured accurately by the models.

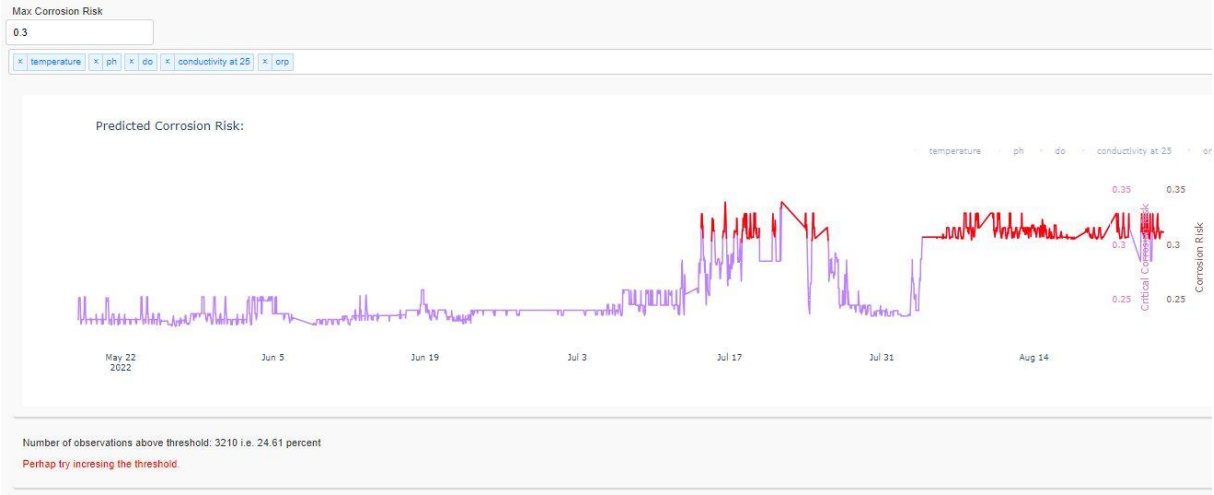

Figure 36: BLUE1, Measurement Campaign 1, Corrosion Risk as calculated using the SOCORRO Application (model trained using Lab data). Threshold set at 0.3.

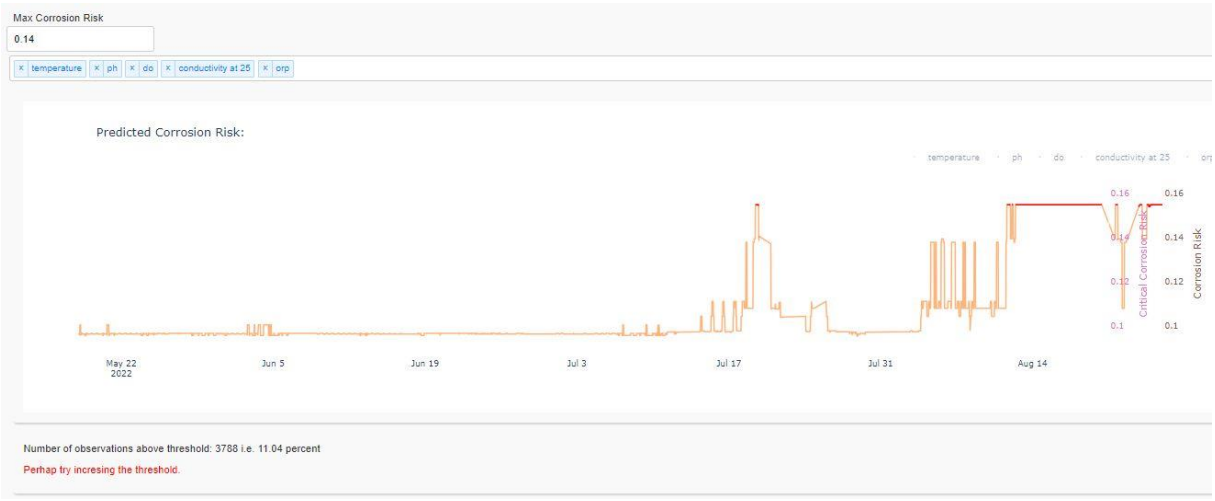

Figure 37: BLUE1, Measurement Campaign 1, Corrosion Risk as calculated using the SOCORRO Application (model trained using Field data). Threshold set at 0.14.

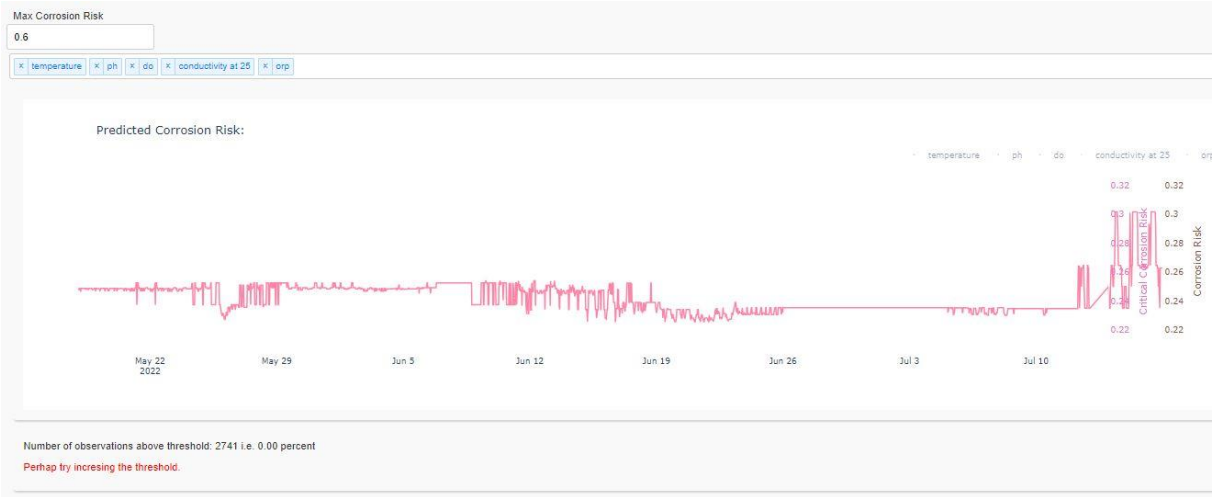

Figure 38: BLUE2, Measurement Campaign 1, Corrosion Risk as calculated using the SOCORRO Application (model trained using Lab data). Threshold set at 0.6.

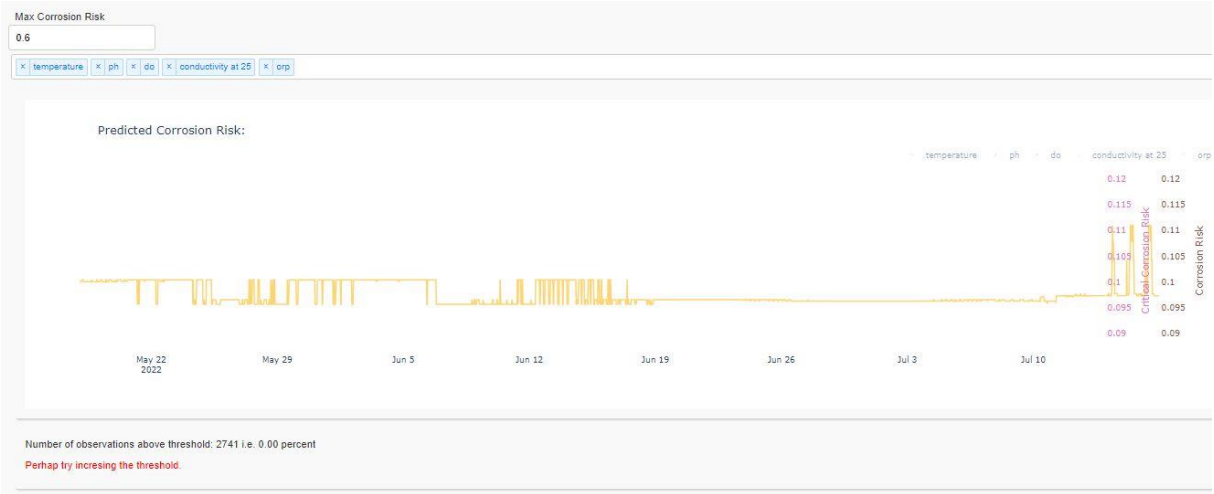

Figure 39: BLUE2, Measurement Campaign 1, Corrosion Risk as calculated using the SOCORRO Application (model trained using Field data). Threshold set at 0.6.

Comparing to the measured corrosion rates as shown in Figure 40, it is clear that the features observed in the results of the SOCORRO App are not observed in the measured data and vice versa. (Note that the SOCORRO App result for BLUE2 only goes up to 16/7.) The reason that the features observed in the COSASCO data are not visible in the result from the SOCORRO App is that the changes in measured corrosion rate are not reflected in changed in the environmental parameters. I.e. these changes are caused by factors not taken into account in the SOCORRO Approach. More specifically, the initially higher corrosion rates are because the clean steel corrodes faster than steel with a protective layer of corrosion products. This time evolution is not captured in the SOCORRO models. The second feature with a strong increase in corrosion rate for BLUE2 at the beginning of August would also not be captured by the model, as this is due to the probe having been above water for 2 days during a maintenance run.

Perhaps more surprising is that for BLUE1, the model predicts two increases in corrosion risk, which are not immediately obvious from the experimental data. However, when looking at the individual measured parameters in more detail, and focussing on the period from 3 July to beginning of August, it can be seen that in this period there is an increase in temperature (Figure 41) starting on 3/7, followed by a peak and again a decrease towards beginning of August. In the pH measurement (Figure 42), a similar trend can be observed, while in the DO measurement (Figure 43), there is a rather sharp increase around 3/7, followed by a gradual decline until beginning of Augusts. The combination of these three parameters, explains why the model predicts a higher corrosion risk for this time period, which from a theoretical point of view is indeed a correct prediction, even if it is not reflected in the experimentally measured corrosion rate. Here, it should be noted that the used ER-probes have a slow response rate, and may not be ideally suited to capture these (on a corrosion scale) short term variations. After the short decline in all these parameters towards the beginning of August, an increase in all three parameters can again be observed as August progresses, which is reflected in the model results as again an increase in corrosion risk.

Although the model will clearly need further refinement, mainly be having more and better training data, the above discussion does show that in general, the proposed approach allows to accurately capture variations in environmental parameters in a corrosion risk.

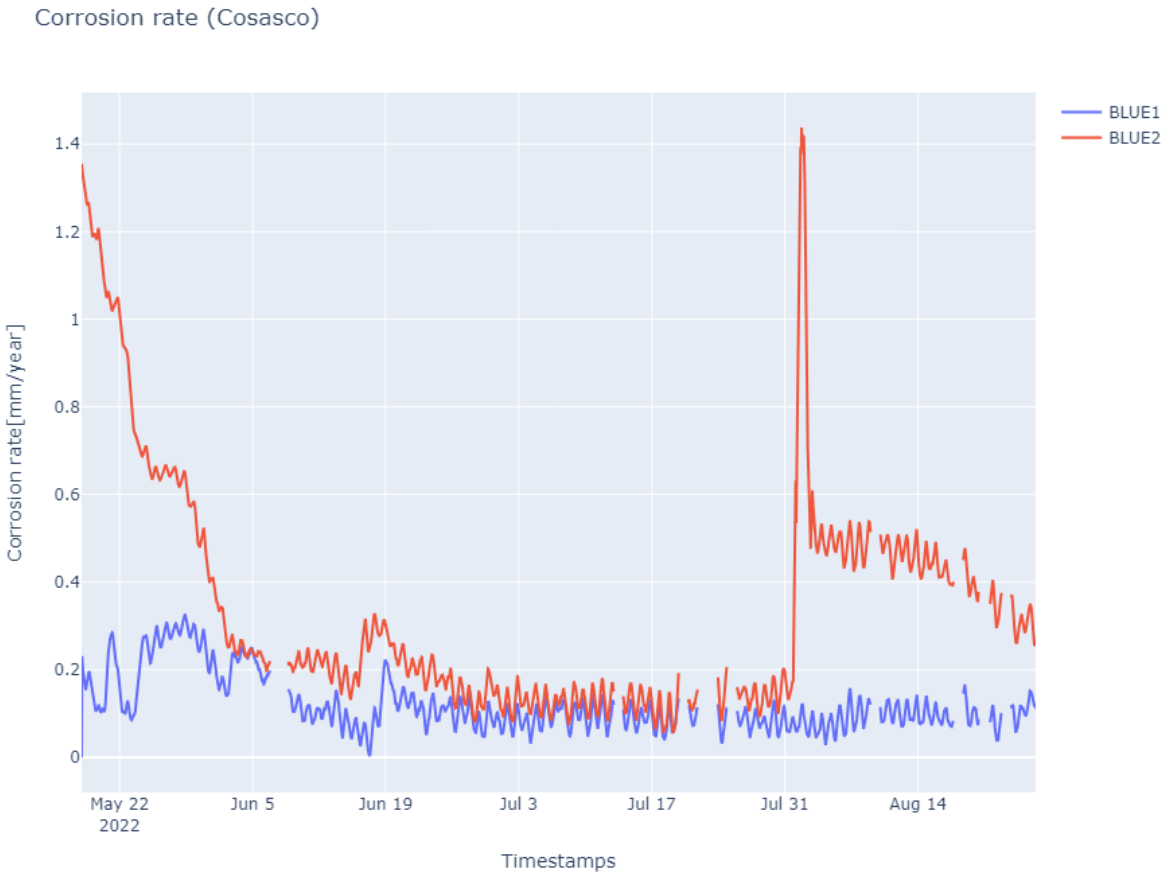

Figure 40: Corrosion rates as measured using COSASCO ER-probes in the period 18/5 to 25/8.

Figure 41: Temperature measured at BLUE1. Data in the period used for analysis by the SOCORRO App.

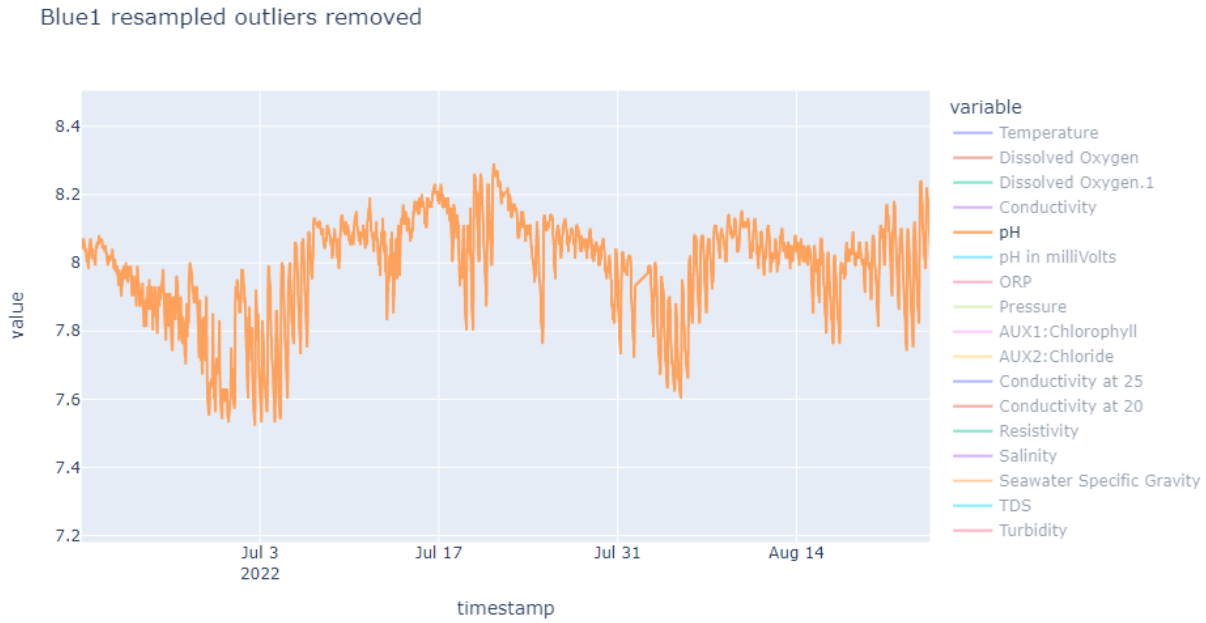

Figure 42: pH measured at BLUE1. Data in the period used for analysis by the SOCORRO App.

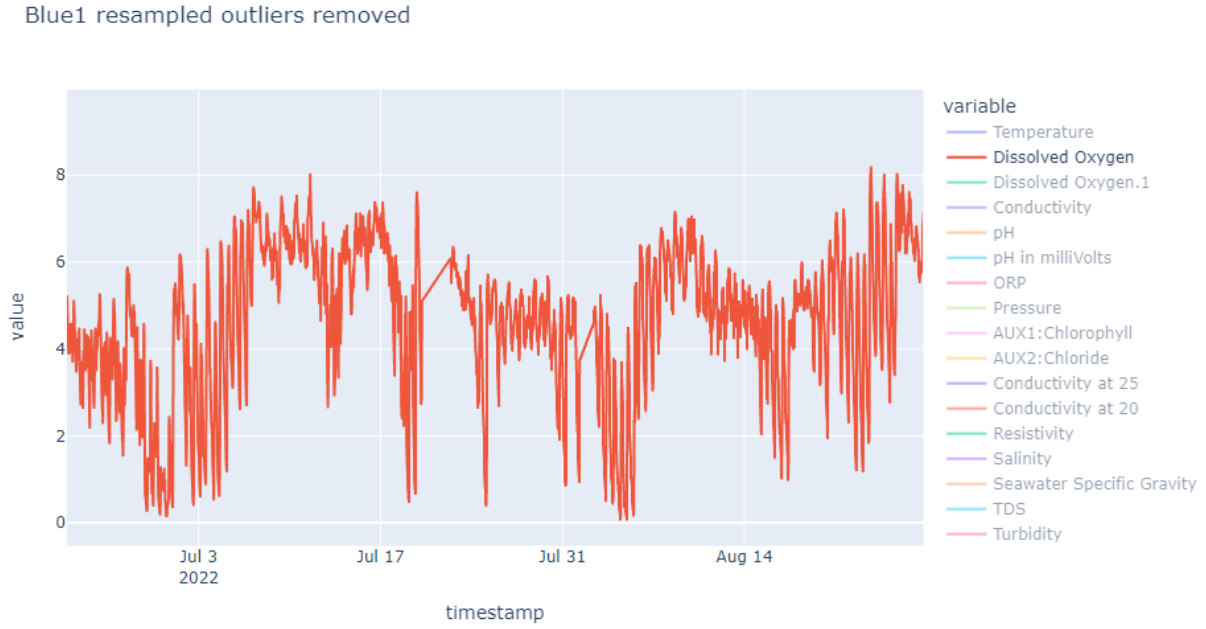

Figure 43: Dissolved Oxygen measured at BLUE1. Data in the period used for analysis by the SOCORRO App.

Measurement campaign 2: 11/03/2023-30/04/2023

Introduction

Starting from February 6th 2023, environmental sensors were again installed at the Blue Accelerator after a long period of maintenance at the sensor supplier. Unfortunately, when installing the external sensors (BLUE2), it became clear that in the time between the first and second measurement campaign, the cable of the sensor which had remained installed at the Blue Accelerator got damaged.

Upon further inspection, a break in the cable was found. It proved impossible to find a short term solution, and the water parameter measurements at BLUE2 had to be abandoned. This section will therefore only focus on the water quality measurements inside the monopile (BLUE1). The relevant corrosion data has already been included in the overview given at the beginning of the Results and Conclusions section. In addition, from February 9 till March 11, there was a problem with the data acquisition system, resulting in a loss of data during that period.

Measured data and observed correlations

The most interesting parameters to study are Dissolved Oxygen (DO), pH, Temperature and Electrical Conductivity (EC). The results of the measurement are shown in Figure 44 to Figure 46. From Figure 44, it can be observed that there is again a very strong correlation between DO and pH, as had also been observed in the first measurement campaign. It is reasonable to assume that this is again linked to biological activity in the monopile, along with the action of tidal water movement. Unfortunately, the reference of external monopile data is missing to verify this. In addition, it can be seen from Figure 45 that the overall drop in Dissolved Oxygen (and pH) corresponds to an increase in the water temperature. An increase in temperature is known to be correlated to a decreasing DO value as the saturation concentration of oxygen in water decreases with increasing temperature. Finally, Figure 46 shows that no clear trend can be observed in the conductivity data.

Looking at the corrosion data presented at the beginning of this section, it can be observed that although changes are occurring in the environmental parameters, there are no changes in the corrosion rate observed. First, this may be due to the slow response rate of the sensors. However, this may also be because the observed trends adversely affect the corrosion rate. The increase in temperature and decrease in pH would increase corrosion rate, while the decreasing DO would reduce the corrosion rate. It may be that these two trends cancel each other out.

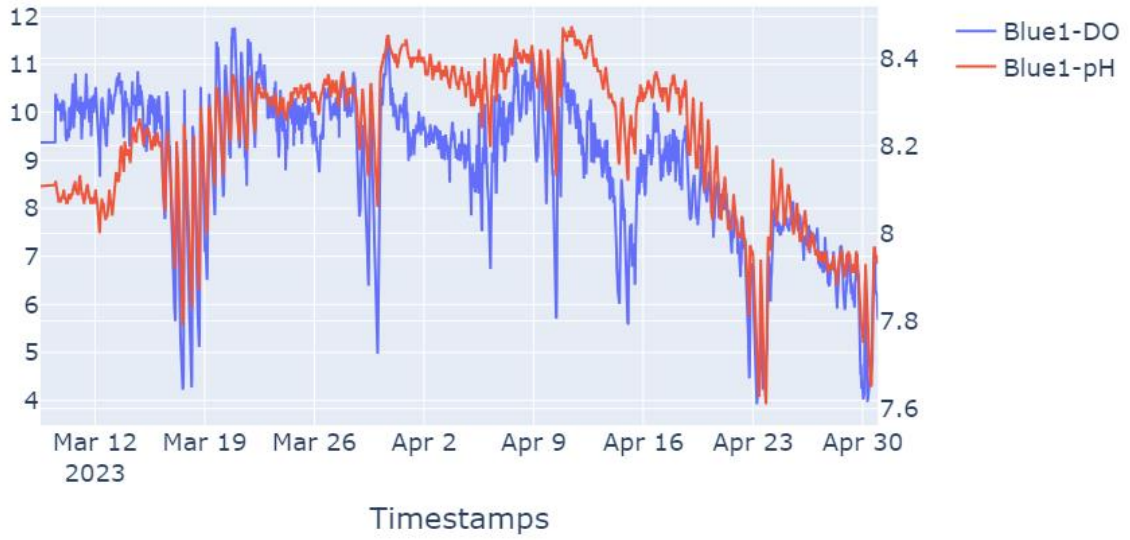

Figure 44: BLUE1. Dissolved Oxygen [mg/l] and pH [-] measurements for Measurement Campaign 2.

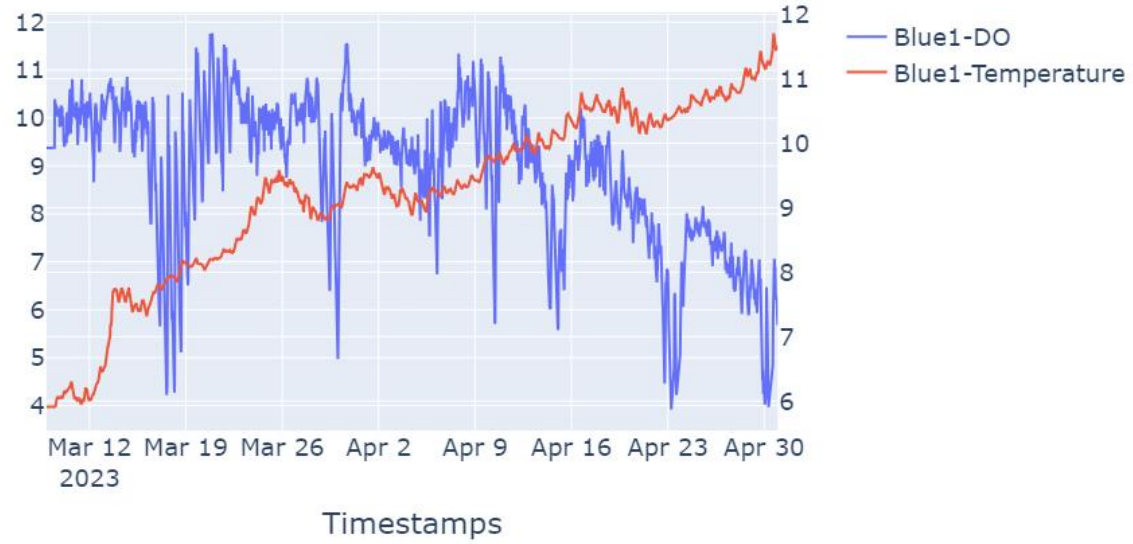

Figure 45: BLUE1. Dissolved Oxygen [mg/l] and Temperature [°C] measurements for Measurement Campaign 2.

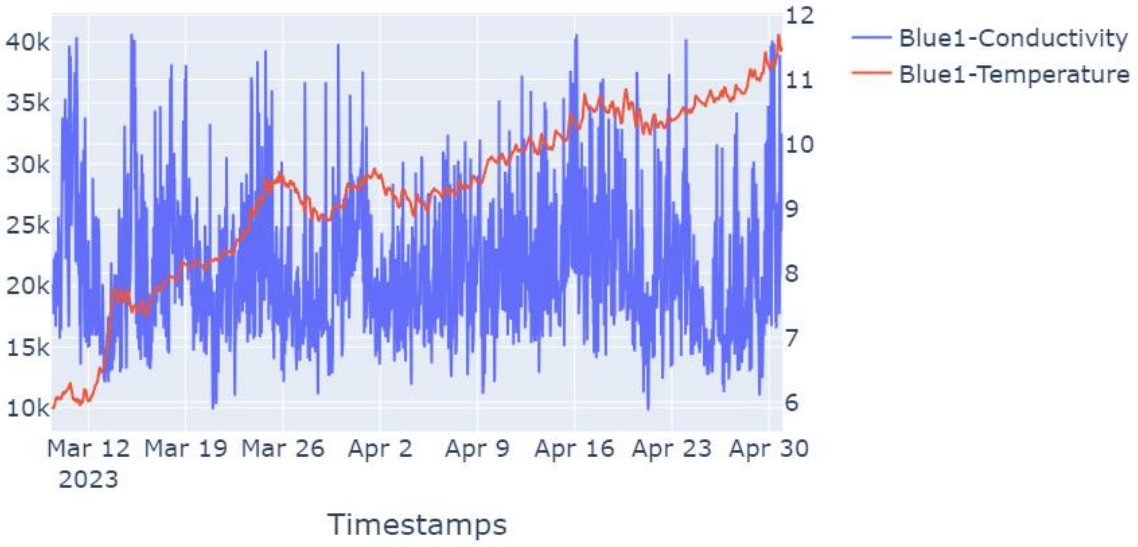

Figure 46: BLUE1. Conductivity [µS/cm] and Temperature [°C] measurements for Measurement Campaign 2.

Plans for further use

Sirris plans to continue and possibly even expand the demonstrator at the Blue Accelerator test site. There are two very tangible trajectories to follow.

(1) On the one hand, the owner of the Blue Accelerator test site (POM West-Vlaanderen) is very happy with the obtained results and would like to see the measurements continued. The data collected is of value for the POM itself, but may also provide data about the conditions at the test site, which can be useful for other companies and research institutes that want to do tests at the Blue Accelerator. We are therefore exploring options to finance continued measurements at the Blue Accelerator. In addition, the POM has asked if the data of the SOCORRO project can be made available on the Blue Accelerator data platform (sensor

dashboard basic - Dashboards - Grafana (vliz.be)). Together with POM West-Vlaanderen, Sirris is currently exploring how this can be achieved from a technical point of view.

(2) Sirris is part of a partnership that has been awarded the Horizon Europe project WILLOW. Within that project Sirris will look into the possibilities to monitor pitting corrosion and coating degradation. Part of the approach and sensor set-up developed within SOCORRO will be used as a starting point for the WILLOW project. The goal is to upgrade the existing monitoring setup based on the lessons learned from SOCORRO, as well as complement it with additional sensors.